ANL/ESD/10-5

Life-Cycle Analysis Results of Geothermal Systems in Comparison to Other Power Systems

Energy Systems Division

ANL/ESD/10-5

Life-Cycle Analysis Results of Geothermal Systems in Comparison to Other Power Systems

by
J.L. Sullivan, C.E. Clark, J. Han, and M. Wang
Center for Transportation Research
Energy Systems Division, Argonne National Laboratory

August 2010

CONTENTS

CONTENTS (CONT.)

FIGURES

FIGURES (CONT.)

TABLES

TABLES (CONT.)

ACKNOWLEDGMENTS

Argonne National Laboratory's work was supported by the U.S. Department of Energy, Assistant Secretary for Energy Efficiency and Renewable Energy, Office of Geothermal Technologies, under contract DE-AC02-06CH11357. The authors wish to express gratitude for the expert assistance of Gregory Mines, Idaho National Laboratory; A.J. Mansure, Geothermal Consultant; and Michael McLamore, Argonne National Laboratory, in our data gathering and modeling efforts. We also thank our sponsor, Arlene Anderson, of Office of Geothermal Technologies, the Office of Energy Efficiency and Renewable Energy, U.S. Department of Energy.

ACRONYMS AND ABBREVIATIONS

Argonne	Argonne National Laboratory
API	American Petroleum Institute
BWR	boiling water reactor
CO_2	carbon dioxide
CTG	cradle-to-gate
EAF	electric arc furnace
EGS(s)	enhanced geothermal system(s)
EIO	economic input/output
EOL	end of life
ESP(s)	electrical submersible pump(s)
EV(s)	electric vehicle(s)
GETEM	Geothermal Electricity Technology Evaluation Model (DOE)
GHG(s)	greenhouse gas(es)
GREET	Greenhouse Gases, Regulated Emissions, and Energy Use in Transportation (Argonne model)
HT	hydrothermal
IGCC	integrated gasification combined cycle
INF	infrastructure (stage)
LCA	life cycle analysis
LCI	life cycle inventory
LHV	lower heating value
MPR(s)	mass-to-power ratio(s)
NG	natural gas
NGCC	natural gas combined cycle
NRC	U.S. Nuclear Regulatory Commission
NREL	National Renewable Energy Laboratory
PCB	pulverized coal boiler
PCA	process chain analysis
PHEV(s)	plug-in hybrid electric vehicle(s)
PV	photovoltaic
PWR	pressurized water reactor

R&D	research and development
RPS(s)	Renewable Portfolio Standard(s)
WTP	well to plant

Units of Measure

bbl	billion barrels
bpm	barrels per minute
Btu(s)	British thermal unit(s)
cm	centimeter(s)
ft	foot, feet
gal	gallon(s)
gpm	gallon(s) per minute
hp	horsepower
hr	hour(s)
in.	inch(es)
kg	kilogram(s)
km	kilometer(s)
kPa	kilo Pascal
kW	kilowatt(s)
kWh	kilowatt-hour(s)
L	liter(s)
m	meter(s)
min	minute
MJ	megajoule(s)
MW	megawatt(s)
psi	pounds per square inch
s	second(s)
yr	year

LIFE-CYCLE ANALYSIS RESULTS OF GEOTHERMAL SYSTEMS IN COMPARISON TO OTHER POWER SYSTEMS

J.L. Sullivan, C.E. Clark, J. Han, and M. Wang

ABSTRACT

A life-cycle energy and greenhouse gas emissions analysis has been conducted with Argonne National Laboratory's expanded Greenhouse Gases, Regulated Emissions, and Energy Use in Transportation (GREET) model for geothermal power-generating technologies, including enhanced geothermal, hydrothermal flash, and hydrothermal binary technologies. As a basis of comparison, a similar analysis has been conducted for other power-generating systems, including coal, natural gas combined cycle, nuclear, hydroelectric, wind, photovoltaic, and biomass by expanding the GREET model to include power plant construction for these latter systems with literature data. In this way, the GREET model has been expanded to include plant construction, as well as the usual fuel production and consumption stages of power plant life cycles. For the plant construction phase, on a per-megawatt (MW) output basis, conventional power plants in general are found to require less steel and concrete than renewable power systems. With the exception of the concrete requirements for gravity dam hydroelectric, enhanced geothermal and hydrothermal binary used more of these materials per MW than other renewable power-generation systems. Energy and greenhouse gas (GHG) ratios for the infrastructure and other life-cycle stages have also been developed in this study per kilowatt-hour (kWh) of electricity output by taking into account both plant capacity and plant lifetime. Generally, energy burdens per energy output associated with plant infrastructure are higher for renewable systems than conventional ones. GHG emissions per kWh of electricity output for plant construction follow a similar trend. Although some of the renewable systems have GHG emissions during plant operation, they are much smaller than those emitted by fossil fuel thermoelectric systems. Binary geothermal systems have virtually insignificant GHG emissions compared to fossil systems. Taking into account plant construction and operation, the GREET model shows that fossil thermal plants have fossil energy use and GHG emissions per kWh of electricity output about one order of magnitude higher than renewable power systems, including geothermal power.

1 INTRODUCTION

Increasing concern over climate change and energy security is driving a call for reducing both fossil carbon emissions and U.S. dependence on foreign oil. Given the nation's growing population, demand for energy will increase in the decades ahead and further fuel these concerns. These circumstances have prompted a renewed national interest in alternative energy resources for application across all of the economic sectors. This interest is directed especially toward the electric power sector. Coupling the renewed interest and Renewable Portfolio Standards (RPSs) of many individual states, the electric power sector is exploring alternatives to conventional fossil-based generating assets and is focusing considerable attention on renewable power technologies. The search for viable technologies could become even more urgent if electric-drive vehicles, such as plug-in hybrid electric vehicles (PHEVs), take hold in the marketplace. Successful penetration of these vehicles into the marketplace would accelerate the growth in added power-generating capacity over and above that already projected on the basis of new demand concomitant with anticipated economic and population growth.

A frequent argument is that if we are to reduce fossil carbon emissions, we must rely more heavily on renewable energy resources for the power delivered to American households, industry, and business. For electric power generation, wind, solar, biomass, and geothermal-based electricity are the choices most frequently considered for new generating capacity in a carbon-constrained world. These options figure prominently in the RPSs of many states, although generally some states are better endowed with the resources needed to support some of these options than are other states. The EIA (2010) projects that renewable electricity, which now represents around 8.5% of U.S. electricity generation, will increase to about 17% by 2035. Although most of this increase is projected to come from additional wind turbines and biomass combustion plants, geothermal electricity generation is estimated to increase by 60% in the same time frame. However, the percentage increase for geothermal generation could rise considerably higher if enhanced geothermal systems (EGSs) technology, which can effectively operate on the more broadly available, lower-temperature geofluids, proves to be a good cost and environmental performer. Coupling EGS technology with the fact that geothermal plants tend both to run "trouble free" at nearly full capacity for most of their lifetimes and to serve base load power demand well, geothermal power, customarily associated with states with conspicuous geothermal resources (geysers, etc.), could become a viable option for many other states and, in the process, become a significant contributor to the U.S. power infrastructure.

There are a number of reasons for enacting the RPSs, including to promote energy diversity, resource conservation, climate change mitigation, reduced air pollution, habitat preservation, energy price stability, new jobs, and others. Environmental considerations are an important component. However, there is a need for a more complete elucidation of environmental performance of geothermal power compared to other power technologies. Whatever choices we make in the future regarding U.S. electricity generation, performing an environmental assessment is an essential part of its evaluation. Historically, life-cycle analysis (LCA) protocols were developed to analyze the environmental performance of consumer products and the processes used to manufacture them. Since then, the LCA's merits as an environmental assessment method had become sufficiently compelling to motivate the

development of an international protocol for LCA (e.g., ISO 14040 [ISO 1997], 14041 [ISO 1998], 14042 [ISO 2000]). For the transportation and energy fields, several LCA models have been developed to represent automobiles and other energy-consuming systems (Wang 1999; Delucchi 2003; CONCAWE/EUCAR/JRC 2007). It is a method that provides a system-wide perspective of a product or service, one that considers all stages of its life cycle, including material production, system manufacture and assembly, service provision, maintenance and repair, and end-of-life processes. Although a number of life-cycle assessments for various types of electricity generation can be found in various databases (e.g., the U.S. life cycle inventory [LCI] database by the National Renewable Energy Laboratory [NREL], most of the energy analysis results are presented for the service provision stage of the plant's life cycle and not for its infrastructure stage — henceforth termed its "plant cycle" stage. Treating the results this way occurs because generally the energy associated with the infrastructure life-cycle stage is small, at least for conventional power plants. However, this assumption may need to be examined for geothermal and other renewable systems, especially considering the former's reliance on both subsurface (e.g., wells) and surface (e.g., pipelines) infrastructure.

The electricity pathway has been an important element in Argonne National Laboratory's (Argonne's) Greenhouse Gases, Regulated Emissions, and Energy Use in Transportation (GREET) Model not only as a process fuel for fuel production but also as a transportation fuel in electric vehicles (EVs) and grid-connected PHEVs (GCPHEVs). Generation efficiencies and plant-site emission factors for combustion technology (residual oil, natural gas, coal, and biomass) are based on Argonne's long history of transportation fuel LCA (see, for example, Wang 1999), while the nuclear and renewable power plants do not produce air emissions at the plant site. The GREET model also takes into account upstream energy and emissions associated with electricity generation from residual oil, natural gas (NG), coal, biomass, and uranium. The major generation technologies in the U.S. power mix are combustion and nuclear, for which the energy use and emissions during the construction of power plants are expected to be negligible compared to those during operation. Therefore, only the service provision stage of the life cycle has been employed for actual energy analysis purposes.

The purpose of this report is to present LCA results derived from our modeling of four geothermal plant types: two EGSs, a hydrothermal binary, and a hydrothermal flash. In particular, the GREET model has been expanded to include power plant construction (as well as plant operation) to address the full life-cycle analysis of different power generation systems. Outputs from the geothermal models are listings of material and energy consumption rates for plant construction and equipment. The listings also include materials and energy consumption associated with the construction and materials composition of wells and their connections to and from plants. Upon integration of the material and energy listings into GREET, life-cycle results are generated for geothermal systems and compared to results extracted from the literature for plant construction so that the life-cycle performance of conventional, geothermal, and other renewable power systems can be compared. A special emphasis is placed on establishing the importance of the plant construction or "infrastructure" stage to the total life cycle for each technology. The life-cycle metrics employed for the comparisons are energy, carbon dioxide (CO_2)-equivalent (CO_2e or CO_2eq) greenhouse gas emissions, and those materials used in significant quantities (typically steel, aluminum, and concrete) for plant construction.

Descriptions of the geothermal models are presented, as is an explanation of the integration of geothermal model output into GREET for the determination of their LCA metrics.

2 METHOD

All life-cycle calculations developed herein are based on process life-cycle assessments, often referred to as process chain analyses (PCAs). More specifically, our approach strictly employs detailed process specific-data that (ideally) are fully speciated, which means that purchased energy units (e.g., liters [L], kilowatt-hours [kWh], cubic meters [m^3], kilograms [kg], tonnes) and specific materials consumption levels (e.g., tons, kg, tonnes) are the data of choice. If these values are not available, however, megajoule (MJ) or British thermal unit (Btu) values are acceptable, although less desirable due to the ambiguity of whether they are high or low heat values or already converted to life cycle values. In a process LCA, all energy and materials flows of each unit process in a production scheme are quantified and combined to represent the entire production or product system. This phase of an LCA is called the LCI analysis. Because of a lack of process LCA data, some authors cited herein employed economic input/output (EIO) energy data for parts of their analyses. EIO is a method that estimates energy and emissions by using economic sector data, which includes the effects of all processes throughout the economy that are not only directly associated with the manufacture of a product but also those that are indirectly associated with it, such as suppliers supplying other suppliers. Because our objective is to compare geothermal and other electricity-generating technologies with as much certainty as possible, process LCA data are used instead of EIO data, as the latter represents economy-wide average performance generally lacking in the process-specific information typically available with the former. However, EIO-derived methods appear to be increasingly employed in LCA studies. Recent discussions of LCA methodologies focus on the so-called attributional LCA vs. consequential LCA. While attributional LCAs are the traditional process-based LCAs, consequential LCAs follow EIO LCA approaches to take into account direct and indirect effects of certain actions. The latter have recently been applied in some biofuel LCAs.

A key component of any life-cycle assessment is a statement of system boundaries. It is difficult at best to compare study results without clearly defined boundaries. A significant component of observed variances between studies arises from differences in system definition.

The system boundary for our study is depicted in Figure 1; the system product is a lifetime of kWh delivered to the grid. As the figure shows, the life-cycle stages defined as "covered" in our study are fuel production, fuel use (plant operation), plant construction, and (lastly) plant decommissioning and recycling. The plant decommissioning and recycling phase makes a small contribution to plant cycle results. As a result, our investigation into geothermal power plants did not include this stage, although some studies of other electricity-generating technologies cited in this report did incorporate this stage. In fact, energy use and emissions from decommissioning and recycling turn out to be a small fraction of the plant cycle burdens, which are, in turn, a small fraction of those for the total life cycle. Regarding the plant cycle or infrastructure stage of the life cycle, our systems boundary is the plant fence line. All assets inside that line are a part of the infrastructure stage of the life cycle. The only exceptions outside this boundary that are to be included are processes required to make the materials and fuels needed to construct assets inside the fence. Some studies broaden the system boundaries. For example, two studies cited herein included NG pipelines, thousands of kilometers in length, in

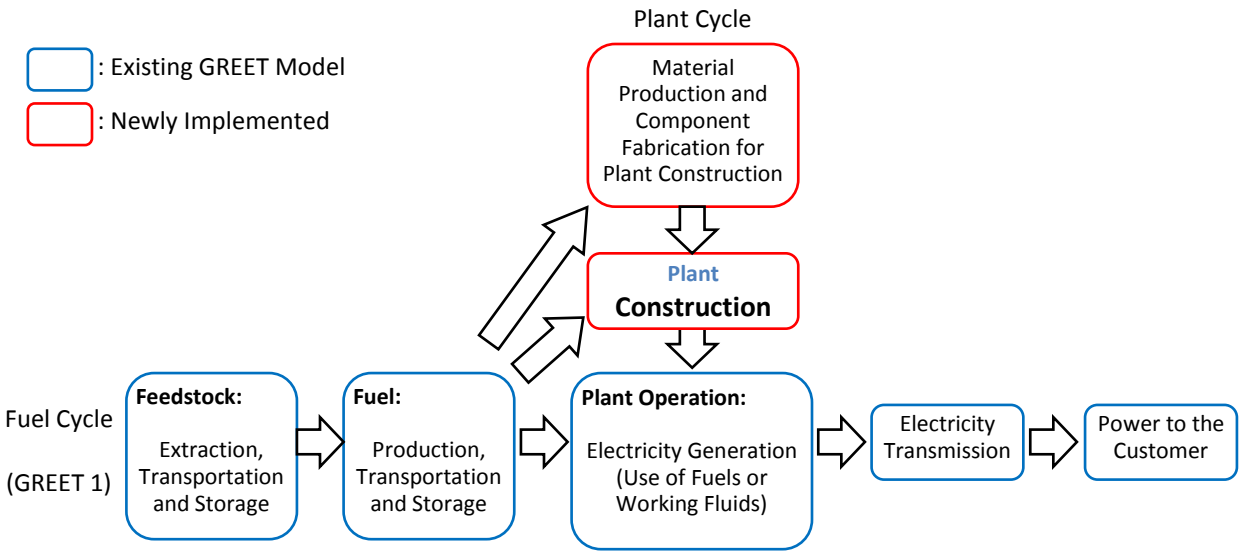

FIGURE 1 Flowchart of Life-Cycle Analysis

the plant stage of the life cycle. While we do not advocate ignoring these assets, they are rightfully a component of the fuel feedstock (well to plant [WTP]) stage of the plant's life cycle, and therefore, the material and energy inputs and outputs associated with the NG pipelines should be allocated to the WTP stage and not to the plant cycle stage. Nonetheless, pipeline operation that uses electricity and/or natural gas is included in our LCAs.

We refer to the construction stage of a power plant's life cycle as the "infrastructure" stage (INF), recognizing that this stage also includes life-cycle burdens incurred in producing a plant's constituent materials (e.g., concrete, steel, aluminum) for plant buildings, enclosures, and equipment (e.g., turbines, generators, heat exchangers) contained therein. In our survey, we track the most significant materials used for power plant construction (e.g., steel and concrete), but we also track other materials that appreciably contribute to the life cycle burdens of power plant construction. Power plant performance characteristics, as well as material compositions, are recorded in Tables 2a, 2b, and 2c for all systems covered herein. They will be discussed later in the report. Material compositional data given in the tables are normalized on a per-megawatt (MW) power output capacity and are henceforth termed mass-to-power ratios (MPRs). For simplicity, in the few cases where energy units are cited, the same label applies, except where the units are different and labeled as such (e.g., liters/MW). The MPRs can be thought of as metrics based on a "hardware functional unit" (i.e., a MW of output capacity). The "service functional unit," a burden (energy and carbon dioxide) per service delivered (MWh), is used later in the report for comparing the life cycle performance of the different generating technologies. This unit reflects plant performance based on both the hardware capacity of the system and how the system is used, as affected by plant lifetime and capacity factor. The net capacity factor of a power plant is the ratio of its actual energy output over a period of time versus its output if it had operated at full nameplate capacity the entire time. The capacity factor of the different plant technologies can be quite variable for the reasons stated in the appropriate sections.

3 GEOTHERMAL LCA MODELING

Currently, geothermal electric power comprises only 0.5% of the electricity generated in the United States and is projected to increase to 0.6% by 2035 (EIA 2010). This small increase certainly does not reflect the research and development (R&D) efforts under way on geothermal technologies, especially EGS technologies. Given the overall doubling of renewable electricity by 2035, geothermal technologies could play an important role in an increase in U.S. renewable electricity in the future. For a resource with this potential, elucidating its environmental performance is a valuable exercise.

For our LCA to cover a representative range of geothermal power plants, four scenarios were developed to assess the potential environmental impacts of geothermal electricity-generation technology. Scenarios 1 and 2 consider two sizes of EGS power plants. Scenario 3 describes a comparatively smaller, binary hydrothermal (HT) power plant. Scenario 4 describes a larger flash hydrothermal power plant. Specific details on each of these facilities are found in Table 1. For labeling purposes, modeling results for these four scenarios are denoted as EGS-20, EGS-50, HT-Binary-10, and HT-Flash-50, respectively.

3.1 GEOTHERMAL POWER PLANTS

Unfortunately, there is a paucity of geothermal life cycle data, including on their material composition, in the literature. For this reason, we elected to analyze the life cycle performance of the geothermal systems included in this study. Four geothermal power systems were examined; more details on the specific geothermal systems are discussed below. Table 2a provides performance and MPR information from both Argonne's analysis and from the literature on the plants, the well field, and the field-to-plant interconnection. For the other power-generating technologies considered here, Tables 2b and 2c provide plant-specific data obtained from available literature. For our geothermal results, two sets of results, generated by using the ICARUS Process Evaluator, were used to provide plant material composition. This evaluator enables estimating of the costs, components, and material requirements for building new production facilities, such as geothermal power plants. A typical ICARUS output is a voluminous list of plant components, equipment, construction costs (material and labor), excavation estimates, and civil engineering requirements. More specifically, the following items are itemized: lengths of pipes of various diameters and wall thicknesses, lengths of wire of various load capacities, numbers of values of different sizes, required pieces of equipment and their weights, amounts of reinforcing bar (rebar), paint, insulation, concrete, cement, and numerous other components. For equipment, constituent types of steel were also given. From tables on pipe and wire sizes (American Petroleum Institute [API] pipe standards and American Wire Gauge wire standards), lengths of pipe and wire were readily converted to masses of steel and copper in the plant associated with those parts. Because steel, cement, concrete, and aluminum make up the bulk of the plant mass, we focused primarily on these materials for our weight estimates. In some cases, approximations needed to be made. For example, the listed weight of a turbine is assumed to be composed entirely of steel.

TABLE 1 Parameter Values for Four Geothermal Power Plant Scenarios

Parameters	Scenario 1	Scenario 2	Scenario 3	Scenario 4
Geothermal Technology	EGS	EGS	Hydrothermal	Hydrothermal
Net Power Output (MW)	20	50	10	50
Producer to Injector Ratio	2	2	3 or 2	3 or 2
Number of Turbines	Single	Multiple	Single	Multiple
Generator Type	Binary	Binary	Binary	Flash
Cooling	Air	Air	Air	Evaporative
Temperature (°C)	150–225	150–225	150–185	175–300
Thermal Drawdown (%/year [yr])	0.3	0.3	0.4–0.5	0.4–0.5
Well Replacement	1	1	1	1
Exploration Well	1	1 or 2	1	1
Well Depth (kilometer [km])	4–6	4–6	<2	1.5 < 3
Pumping	Injection and production	Injection and production	Injection and production	Injection only
Pumps, Injection	Surface	Surface	Surface	Surface
Pumps, Production	Submersible 10,000 feet (ft)	Submersible 10,000 ft	Lineshaft or submersible	None
Distance between Wells (m)	600–1,000	600–1,000	800–1,600	800–1,600
Location of Plant to Wells	Central	Central	Central	Central
Geographic Location	Southwestern United States	Southwestern United States	Southwestern United States	Southwestern United States
Plant Lifetime (yr)	30	30	30	30

3.2 GEOTHERMAL WELL FIELD

This section describes the assumptions and methodologies used to represent the well fields for our scenarios. Table 1 shows the scenarios across several design parameters, which affect performance, cost, and environmental impacts. Each scenario provided input parameters for the U.S. Department of Energy's Geothermal Electricity Technology Evaluation Model (GETEM), and each scenario was run multiple times in GETEM to create a range of possible outcomes.

3.2.1 Well Field Development

To model the well field, it was assumed that the production wells and injection wells would have the same configuration and depth. The components included in the inventory for each well are depicted in Figure 2.

TABLE 2a Plant Details and Material Requirements per MW for Various Geothermal Generating Technologies (Note: mt denotes metric tons - tonnes; first four are modeling results; the remainder are from the literature)

Ref #		Capacity (Cap.) MW	Lifetime Yr	Cap. Factor %	Aluminum mt/MW	Concrete mt/MW	Cement mt/MW	Bentonite mt/MW	Diesel liters/MW	Iron mt/MW	Steel mt/MW	Total mass mt/MW
		Geothermal -- EGS										
EGS-20	Plant	20	30	95	45.2	460				3.9	221	
	Well[a]						971	283	253,000		968	
	Well to Plant[b]						17		10,930		17	
	Totals				45.2	460	988	283	263,930	3.9	1,206	2,713
EGS-50	Plant	50	30	95	42.6	460				2.8	193	
	Well[a]						970	282	229,600		967	
	Well to Plant[b]						17		10,900		15	
	Totals				42.6	460	987	282	240,500	2.8	1,175	2,677
		Hydrothermal - Binary										
HT-Binary-10	Plant	10	30	95	46.1	459				4.28	231	
	Well[c]						71.7	34	38,980		109	
	Well to Plant[d]						16		10,221		16	
	Totals				46.1	459	87.4	34	49,201	4.28	356	964
		Hydrothermal - Flash										
HT-Flash-50	Plant	48.4	30	95		159				1.6	26.1	
	Well[e]						217	77	48,970		255	
	Well to Plant[d]						15		10,040		14	
	Totals					159	232	77	59,010	1.6	295	698
Rule, 2009		162	100	93	21.2	1,883	777[f]		208,000		566	3,249
Frick, 2010	Plant	0.925	30			41.5					292	
	Well[a]						59.9		1,750,000		846	
	Well to Plant[b]											
	Totals					41.5	59.9		1,750,000		1,138	1,239

[a] 6-km well with 3 liners.
[b] 1,000 m of piping assumes half of amount used from production well to the plant and the other half from plant to injection wells.
[c] 1.5-km well, including an exploration well.
[d] 1,000 m of piping.
[e] For 2.5-km well, including exploration well.
[f] Insulation glass.

TABLE 2b Plant Details and Material Requirements per MW for Three Conventional and One Renewable Generating Technologies (Note: mt denotes metric tons – tonnes)

Ref #	Capacity MW	Lifetime Yr	Cap. Factor %	Aluminum mt/MW	Concrete mt/MW	Cement mt/MW	Cu mt/MW	Si mt/MW	Pb mt/MW	Iron mt/MW	Steel mt/MW	Total Mass mt/MW
			Coal									
Pacca, 2002	913	30	70	0.68	195						68.2	264
Spath, 1999	360	30	60	0.42(.004)[a]	159					0.62	50.7(0.06)[a]	210
White, 1998	1,000	40	75	0.26	74.3		0.45				40.3	115
			NGCC									
Pacca, 2002	875	30	72.4	0.26	81.4						58.5	140
Spath, 2000	505	30	80	0.20	97.8					0.62	31(218)[a]	129
Meier, 2000	620	40	75	0.00	47.7					0.12	2.5(30.1)[a]	50
			Nuclear									
Bryan, 1974[b]	1,000	40	75	0.018	180		0.69		0.46	1.30	42.6	225
NUREG, 2000[c]	1,155	40	75	0.061	307		0.60				29.5	337
			Hydroelectric									
Pacca, 2002	1,296	100	50	0.052	7,644		0.069				24.8	7,669
Hondo, 2005	10	30	45		552							552
Rule, 2009	432	100	50		6,680		1.502				54.5	6,736

[a] Material for either gas pipelines or coal cars.
[b] Pressurized water reactor (PWR).
[c] Boiling water reactor (BWR).

TABLE 2c Plant Details and Material Requirements per MW for Renewable Electricity-Generating Technologies (Note: mt denotes metric tons – tonnes)

Ref #	Capacity MW	Lifetime Yr	Cap. Factor %	Aluminum mt/MW	Concrete mt/MW	Glass mt/MW	Cu mt/MW	Si mt/MW	Plastic mt/MW	Iron mt/MW	Steel mt/MW	Total Mass mt/MW
			Wind									
Pacca, 2002	2,688	20	23.6	2.330	471.0	1.83	0.58		7.5		108.0	595
White, 1998b	25	25	24.0		397.0		0.21		19.9	17.2	59.0	493
White, 1998a	25	25	24.0		305.0		0.21		19.9		84.6	410
Vestas 2006[a]	1.65	20	40.8	1.700	443.0	14.8	1.59		1.6	16.1	102.0	583
Vestas 2006[b]	300	20	40.8	4.770	443.0	14.8	2.48		6.4	16.1	102.3	592
Rule, 2009	91	100	45.0	4.180	526.0	29.4	20.10		19.5		222.0	821
Schleisner, 2000	9	20	25	2.8	565	2.2	0.7		4		129	704
			Photovoltaic									
Pacca, 2002	4,118	30	15.4	43.2	540[c]	259.	117				1,117	2,076
Mason, 2006	3.5	30	19.7	19.0	65.7		7.53		5.8		55.9	160
Phylipsen, 1995	1	25	15.6	11.4		45.5	0.17	2.510	14.2			74
de Wild-, 2005	1	25	15.6	23.0		69.1	0.85	4.520	7.9			105
			Biomass									
Biomass-88	88.5	30	88.2	1.3	159					0.9	51(14)[d]	

[a] For a single 1.65-MW turbine only.
[b] For 182 turbines, each with 1.65-MW capacity plus grid connection.
[c] Cement.
[d] Steel for the trucks to deliver the biomass to the plant.

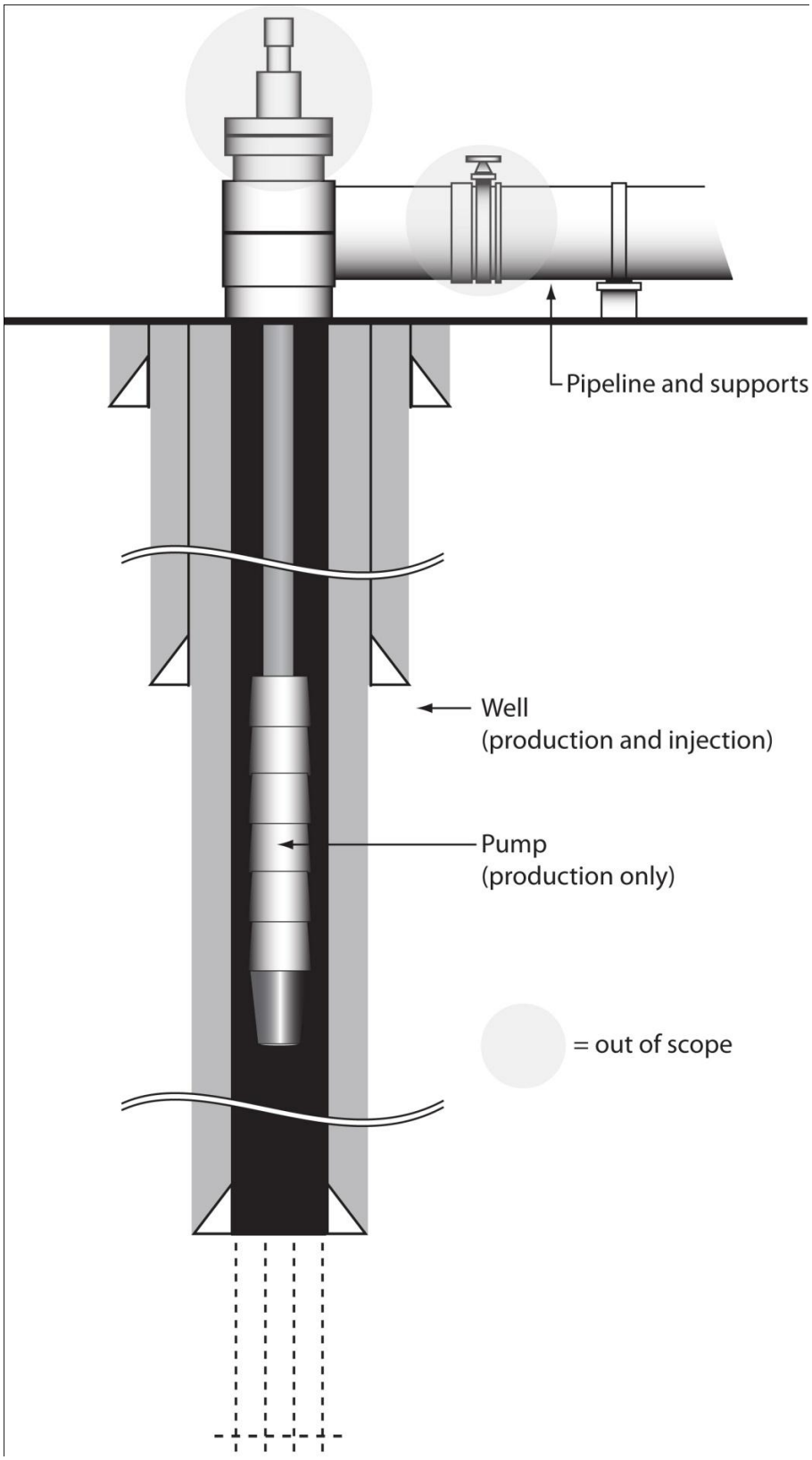

FIGURE 2 System Boundary of Individual Geothermal Well in the Well Field

For Scenarios 1 and 2, the well designs were based on the 5,000-m EGS wells described in *The Future of Geothermal Energy: Impact of Enhanced Geothermal Systems (EGS) on the United States in the 21st Century* (MIT 2006). This design was modified to assess material requirements for wells at various depths. Summaries of each modified design are provided in Table 3a.

TABLE 3a Well Characteristics for EGS Power Plant Scenarios 1 and 2

Well Depth (km)	Casing Schedule	Material	Depths (m)	Length (m)	Hole (cm)	Casing (cm)	Weight/length (kg/m)
4	Conductor Pipe	Welded wall	24	24	91.44	76.20	176
	Surface Casing	Welded wall	381	381	66.04	55.88	219
	Intermediate Liner	K-55 Premium	1,524	1,204	50.80	40.64	162
	Production Casing	T-95 Premium	3,249	3,249	37.47	29.85	97
	Production Slotted Liner	K-55 Buttress	3,999	811	26.99	21.91	54
5	Conductor Pipe	Welded wall	24	24	91.44	76.20	176
	Surface Casing	Welded wall	381	381	71.12	55.88	219
	Intermediate Liner	K-55 Premium	1,524	1,204	50.80	40.64	162
	Production Casing	T-95 Premium	3,999	3,999	37.47	29.85	110
	Production Slotted Liner	K-55 Buttress	4,999	1,061	26.35	21.91	54
5	Conductor Pipe	Welded wall	30	30	106.68	91.44	215
	Surface Casing	Welded wall	381	381	81.28	71.12	390
	Intermediate Liner #1	Welded wall	1,524	1,204	66.04	55.88	306
	Intermediate Liner #2	L-80 Buttress	2,743	1,280	50.80	40.64	190
	Production Casing	T-95 Premium	3,999	3,999	36.20	29.85	120
	Production Slotted Liner	K-55 Buttress	4,999	1,061	26.04	21.91	54
6	Conductor Pipe	Welded wall	30	30	106.68	91.44	215
	Surface Casing	Welded wall	381	381	81.28	71.12	390
	Intermediate Liner #1	Welded wall	1,524	1,204	66.04	55.88	306
	Intermediate Liner #2	L-80 Buttress	3,048	1,585	50.80	40.64	190
	Production Casing	T-95 Premium	4,999	4,999	36.20	29.85	120
	Production Slotted Liner	K-55 Buttress	5,998	1,061	26.04	21.91	54
6	Conductor Pipe	Welded wall	30	30	152.40	132.08	827
	Surface Casing	Welded wall	381	381	121.92	106.68	668
	Intermediate Liner #1	Welded wall	1,524	1,204	91.44	76.20	418
	Intermediate Liner #2	Welded wall	2,591	1,128	71.12	60.96	334
	Intermediate Liner #3	L-80 Buttress	3,658	1,128	50.80	40.64	190
	Production Casing	T-95 Premium	4,999	4,999	36.20	29.85	120
	Production Slotted Liner	K-55 Buttress	5,998	1,061	26.04	21.91	48

For the binary and flash HT systems, a different well design configuration was used. The design for these wells was based upon well RRGE2 in Raft River, Idaho (Narasimhan and Witherspoon 1977); see Table 3b for details.

TABLE 3b Well Characteristics for Hydrothermal Power Plants in Scenario 3 (depth less than 2 km) and Scenario 4 (depth between 1.5 and 3 km)

Well Depth (km)	Casing Schedule	Material	Depths (m)	Length (m)	Hole (cm)	Casing (cm)	Weight/length (kg/m)
0.67	Conductor Pipe	Welded wall	24	24	91.44	76.20	176
	Surface Casing	K-55 Buttress	152	152	66.04	50.80	251
	Production Casing	K-55 Premium	457	457	44.45	34.73	122
	Production Slotted Liner	K-55 Buttress	610	213	31.12	24.45	80
1	Conductor Pipe	Welded wall	24	24	91.44	76.20	176
	Surface Casing	K-55 Buttress	152	152	66.04	50.80	251
	Production Casing	K-55 Premium	695	695	44.45	34.73	122
	Production Slotted Liner	K-55 Buttress	1,000	366	31.12	24.45	80
1.5	Conductor Pipe	Welded wall	24	24	91.44	76.20	176
	Surface Casing	K-55 Buttress	152	152	66.04	50.80	251
	Production Casing	K-55 Premium	1,042	1,042	44.45	34.73	122
	Production Slotted Liner	K-55 Buttress	1,500	518	31.12	24.45	80
2	Conductor Pipe	Welded wall	24	24	91.44	76.20	176
	Surface Casing	K-55 Buttress	152	152	66.04	50.80	251
	Production Casing	K-55 Premium	1,390	1,390	44.45	34.73	122
	Production Slotted Liner	K-55 Buttress	1,999	671	31.12	24.45	80
2	Conductor Pipe	Line Pipe	24	24	121.92	101.60	239
	Surface Casing	X-56, Line Pipe	152	152	91.44	76.20	234
	Intermediate Liner	K-55 Buttress	762	671	66.04	50.80	251
	Production Casing	K-55 Premium	1,390	1,390	44.45	34.73	122
	Production Slotted Liner	K-55 Buttress	1,999	671	31.12	24.45	80
2.5	Conductor Pipe	Line Pipe	24	24	121.92	101.60	239
	Surface Casing	X-56, Line Pipe	152	152	91.44	76.20	234
	Intermediate Liner	K-55 Buttress	1,067	975	66.04	50.80	251
	Production Casing	K-55 Premium	1,890	1,890	44.45	34.73	122
	Production Slotted Liner	K-55 Buttress	2,499	671	31.12	24.45	80
3	Conductor Pipe	Line Pipe	24	24	121.92	101.60	239
	Surface Casing	X-56, Line Pipe	152	152	91.44	76.20	234
	Intermediate Liner	K-55 Buttress	1,067	975	66.04	50.80	251
	Production Casing	K-55 Premium	2,390	2,390	44.45	34.73	122
	Production Slotted Liner	K-55 Buttress	2,999	671	31.12	24.45	80

The well designs in Tables 3a and 3b were used to determine the amounts of materials, water, and fuel required in the drilling, casing, and cementing of a well. The assumptions and methods used for each phase are described in detail in a companion report (Clark et al. 2010).

3.2.2 Drilling: Fuel and Fluids

The drilling phase of the geothermal power plant life cycle requires heavy equipment, such as drill rigs, fuel, materials, and water. The assumptions and materials used in well construction are described in Sections 3.2.3 and 3.2.4.

To determine the amount of fuel consumption per day required for drilling, the following assumptions were made:

- The drill rig operates with a 2,000-horsepower (hp) engine,
- The engine consumes diesel fuel at a rate of 0.06 gallon (gal)/hp/hour (h), and
- The drill rig runs at 45% of capacity.

These assumptions are similar to those reported by Tester et al. (2006), EPA (2004), and Radback Energy (2009). These assumptions result in a fuel consumption rate of 1,296 gal/day (4,906 L/day) according to the following equation:

$$\text{Fuel Consumption[gal/day]} = 0.45[\text{h/h}] \times 2000[\text{hp}] \times 0.06[\text{gal/hp-h}] \times 24[\text{h/day}]$$

It should be noted that fuel estimates can vary depending upon the size of the rig. In work for Sandia National Laboratories, ThermaSource estimated fuel consumption according to well data and the use of a 3,000-hp rig with a top drive to be 2,500 gal per day, which is higher than our estimate (Polsky 2008, Polsky 2009, Mansure 2010). For the EGS scenarios, the number of days to drill and construct wells was taken from examples in Tester et al. (2006). For the hydrothermal scenarios, the number of days to drill and construct these wells was estimated by using a linear fit to the four string wells described in Tester et al. (2006).

During drilling, fluids or muds lubricate and cool the drill bit to maintain downhole hydrostatic pressure and to convey drill cuttings from the bottom of the hole to the surface. To accomplish these tasks, drilling muds contain chemicals and constituents to control such factors as density and viscosity and to reduce fluid loss to the formation. The total volume of drilling muds depends on the volume of the borehole and the physical and chemical properties of the formation. The composition of the mud was provided by ChemTech Services as summarized by Mansure (2010) and Clark et al. (2010) to provide the required drilling fluid properties. Materials included bentonite, soda ash, gelex, polypac, xanthum gum, polymeric dispersant, high-temperature stabilizer, and modified lignite or resin. As the dominant material by several orders of magnitude is bentonite, the other materials were ignored for the purposes of this study.

3.2.3 Well Casing

In the well design work of Tester et al. (2006), the larger-diameter casings are specified according to grade and thickness rather than grade and weight per foot, which is the customary method per the API (Mansure 2010). Specification accounts for adequate burst, collapse, and yield strength. For any given grade, the thickness specifies the casing design. The weight per foot and inner diameter can be determined from the thickness and grade.

3.2.4 Cementing of Casing

The volume of cement needed for each well was determined by calculating the total volume of the well and the volume of the casing and interior. It was assumed that Class G Cement (according to API Specification 10A) and Class G Cement with 40% silica flour would be used. Silica flour and Portland cement are both accounted for in each well design and depth.

3.2.5 Pumps

For the EGS scenarios and the hydrothermal binary scenario, both production pumps and injection pumps are needed. It is assumed for the hydrothermal flash scenario that only injection pumps are needed. For the purposes of this study, the surface pumps are attributed to the power plant material inventory. Only the production pumps are affiliated with the well field. Pump requirements were determined from scenario runs in GETEM. Two types of pumps, the electrical submersible pump (ESP) and the lineshaft pump, were considered where feasible. Table 4 presents the material requirements for a single downhole pump for a production well according to the specifications of each scenario. As lineshaft pumps are limited by well depth, only the binary scenario could use either a lineshaft pump or ESP.

TABLE 4 Material Requirements for One Downhole Pump According to Scenario Requirements

Scenario Pump Configuration	Steel (Mg)	Copper (Mg)	Brass (Mg)	Lead (kg)	Oil (kg)	Rubber (kg)
EGS ESP	8.4 - 30.3	1.0 - 2.2	0.5 - 0.6	0.5 - 0.9	18.1 - 20.4	199.0 - 559.2
Binary ESP	14.0 - 24.0	1.3 - 1.9	0.5 - 0.6	0.5 - 0.9	18.1 - 20.4	349.1 - 437.8
Binary lineshaft	42.2	1.6	1.2	0	45.4	453.6

3.2.6 Hydraulic Stimulation of the Resource

Stimulation of the resource was only considered for the EGS well fields (i.e., Scenarios 1 and 2). Stimulation opens existing spaces within the formation to enable or enhance the circulation of the geofluid. During stimulation, water is pumped down the well hole at a certain pressure and rate to enable the opening of existing spaces. Typically, stimulation occurs at the point of injection to complete the flow of the geofluid from the injection well to a production well. Published information on EGS stimulation projects and the volume of fluid used is limited, and available literature values are from international projects with different geological characteristics than potential U.S. projects. Literature values were used to determine fuel consumption attributable to hydraulic stimulation. See Clark et al. (2010) for water volume estimates.

According to the literature, the average highest flow rate achieved during stimulation is 97 L/second (s) (36.6 barrels [bbl]/minute [min]) (Asanuma et al. 2004; Michelet and Toksöz 2006; Zimmermann et al. 2009). Fuel consumption was determined by using the average highest

flow rate and from industry input. Assuming that the average diesel consumption per pump is 0.13 L/s (2 gallons per minute [gpm]) and that the average pump can move 1.4 m^3/min (9 barrels per minute [bpm]) of stimulation fluid, the fuel consumption per stimulation job is assumed to be 118.5 m^3 (31,300 gal). Fuel consumption will vary according to the characteristics of the resource, the size of the pumps, and the desired characteristics of the designed reservoir.

3.2.7 Pipelines between Wells and Plant

In addition to well construction, infrastructure is needed to deliver the geofluid to the power plant. While the materials at the wellhead are not specifically included in the inventory as shown in Figure 2, the pipeline connecting a well to the power plant is included. For this study, it was assumed that each production well has a separate pipeline to deliver the geofluid through the plant (power plant infrastructure is tracked separately) and to an injection well. As the producer-to-injector ratio is greater than 1, the injection well receives multiple pipelines of produced geofluid. The pipelines are aboveground and require support structure. The approach to determining the materials and energy required for construction and installation of the pipeline is summarized below.

3.2.8 Pipeline

To determine the material requirements for the pipeline, the diameter of the pipes were determined first according to the distance between the wells, flow rate of the geofluid, and physical properties of the geofluid. Assuming a pressure drop of 10 pounds per square inch (psi) (68.95 kPa) and a pipeline distance of 1,000 m, the temperature and flow rate were varied to determine the diameter of the pipe according to the Hagen-Poiseuille equation:

$$\Delta P = \frac{128 \mu L Q}{g \pi D^4}$$

where ΔP is the pressure drop along the pipe in pounds per square feet, L is the length of pipe in feet, D is the inside pipe diameter in feet, Q is the volumetric flow rate in cubic feet per hour, μ is the viscosity of the geofluid in pounds per hour-foot, and g is the gravitational acceleration in feet per square hour (417,312,000 ft/h^2). According to the scenarios run in GETEM, schedule 40 steel pipe with either an 8-inch (in.) or 10-in. (20.32-centimeter [cm] and 25.40-cm, respectively) diameter would suffice for all scenarios.

3.2.9 Pipeline Supports

For the pipeline supports, 8-in. diameter, schedule 40 steel pipe was assumed given that the maximum span between supports, 5.8 m (19 ft), is less than the span required for 10-in. diameter pipe — 6.7 m (22 ft) — and therefore, this assumption provided a conservative estimate of material requirements for the support system (McAllister 2009).

The material requirements for the support system include forming tubes, concrete, and rebar for the foundation, and steel for the structural support. Insulation was used at support contacts in addition to the length of pipe from the production well to the power plant. The design for the foundation assumed a hole with a depth of 1.83 m (6 ft) and a diameter of 40.64 cm (16 in.) (E-Z Line 2005). The foundation is composed of a forming tube and concrete interspersed with 6 steel rebar of 1.27-cm (0.5-in.) diameter and 30.48 cm (12 in.) in length. The diameter of the foundation tube was assumed to be 40 cm (15.75 in.) (Sonoco 2008). Concrete mixes can vary considerably in their makeup. Three recipes for controlled low-strength material concrete were selected (IDOT 2007). Two of the three recipes included fly ash (class C or F) in addition to Portland cement, fine aggregate, and water (IDOT 2007). Table 5 summarizes the material requirements (not including water) of the three mixes for one pipeline from a production well to the plant and to an injection well.

TABLE 5 Material Requirements for Concrete Mix for Foundation Supports for a 1,000-m Pipeline

	Recipes for concrete support foundation for 1000 m surface pipeline		
Materials	Mix 1	Mix 2	Mix 3
Portland Cement (Mg)	1.2	2.9	0.9
Fly Ash - Class C or F (Mg)	2.9	0.0	2.9
Fine Aggregate - Saturated Surface Dry (Mg)	68.2	58.8	58.8

It is worth noting that all recipes require the addition of water. Water volumes are tracked and discussed in a separate report by Clark et al. (2010).

3.2.10 Pipeline Insulation

While insulation is used for geothermal pipelines, it is not used consistently throughout a pipeline system. For this study, it was assumed that pipelines are insulated from the production well to the power plant and at every support point. Insulation segment for pipelines are typically 0.94 m (36 in.) in length and average 6 kg per linear meter (4 pounds per linear foot) for pipelines that are 20.32–25.40 cm (8–10 in.) in diameter. Materials used for insulation are often a form of fiberglass with a finished exterior. Additional exterior protection can include metal cladding, although this material was not considered in this analysis.

3.2.11 Pipeline Installation

There are several steps to constructing and installing a pipeline successfully. Although the steps can be run in parallel to reduce the total time spent at a site, diesel-consuming

equipment (e.g., hydraulic excavators and pipelayers) is required for each stage. For the purposes of installing the designed pipeline, it was assumed that medium-sized equipment would be used and that the engines would have a maximum of 268 hp (200 kW) according to equipment specifications (Caterpillar 2009). While medium-sized pipelayers have a somewhat lower maximum horsepower rating than do excavators (i.e., 240 hp versus 268), the higher rating was applied for general fuel consumption during pipe installation activities to arrive at a conservative (larger) estimate of fuel consumption. It was also assumed that the equipment would run at 70% capacity during an 8-hour work day, or 23% capacity for 24 hours. Using the same equation as that used to determine fuel consumption for drill rigs (Radback Energy 2009), the fuel required to run one piece of equipment for pipeline construction at specified capacity and horsepower levels results in a daily fuel consumption rate of 90.5 gal/day (340.9 L/day):

$$\text{Fuel Consumption[gal/day]} = 0.23[\text{h/h}] \times 268[\text{hp}] \times 0.06[\text{gal/hp-h}] \times 24[\text{h/day}]$$

The first step in pipeline construction is to dig the holes and pour the concrete foundation for the support structure. This step is carried out using a hydraulic excavator, and according to estimates by industry experts, it was assumed that digging and pouring one hole takes approximately 45 minutes, so 10 holes can be completed in a given work day. After a hole is dug and poured and the concrete has hardened, the supports are installed. The supports must be aligned carefully to aid pipeline installation. As a result, it typically takes approximately 1.5 hours to install a support; thus, 5 supports can be completed in a given work day. Prior to installing the pipeline, each section of pipe must be insulated. For the production-to-plant side of the pipeline, the entire length of pipe is insulated, whereas only the length at the point of support is insulated along the plant-to-injection well section. While the insulation is being installed, a pipelayer is used to elevate the pipe section. Practitioners estimate that approximately three to four sections of insulation can be installed per hour. Assuming three sections per hour, approximately 22 sections can be installed per work day.

After the insulation has been installed, the pipeline is secured to the support structures. The pipeline installation can be completed in several ways. Using one pipelayer, it can take 1.5 hours to lay 6.1–12.2 m (20–40 ft) of pipe, or 30.5–61.0 m (100–200 ft) of pipe per day. Using two pipelayers, longer lengths of pipe can be laid, thereby increasing the rate at 1.5 hours to 24.4 m (80 ft) of pipe, or 122 m (400 ft) of pipe per day. Using the 90.5 gal/day (340.9 L/day) consumption rate, to complete a single 1,000-m pipeline, between 37,760–43,354 L (9,975–11,453 gal) of diesel would be required.

For the geothermal scenarios described in Table 1, material composition results for plants and well fields derived from our plant and well field modeling efforts using ICARUS and GETEM models have been included in Table 2a.

3.3 MATERIAL COMPOSITION RESULTS FOR GEOTHERMAL POWER FACILITIES

An inspection of Table 2a shows significant differences in the MPRs for steel, concrete, and cement across scenarios. To aid the reader's review of the data, steel and cement results are depicted in Figure 3. It is clear from the figure that more steel and cement are used in the EGS systems than are used in the hydrothermal scenarios. The primary reason for this result is the design of the wells, as the EGS wells are much deeper than the hydrothermal wells, and thus, the EGS wells require considerably more steel and cement than their hydrothermal counterparts. Temperature of the resource also plays an important role in this case. For a given power output, a lower-temperature resource, typical for EGSs (see Table 1), requires greater fluid flow, which implies an increase in the number of wells. It is also clear from the figure that binary systems, which include EGS, require more steel and cement for concrete in-plant construction than do conventional hydrothermal systems. This result occurs primarily because of large air cooled condensers and the associated piping required to cool large volumes of comparatively low-temperature fluid. (Note that in Figure 3, concrete use is listed for the plant and cement for the wells). The cement content varies greatly according to the application. Finally, notice in Table 2a that considerably more diesel fuel is required for EGS systems than for hydrothermal. Again, this result is a consequence of the deeper wells used for EGS. Admittedly, elements missing from Tables 2a–2c are diesel fuel and other direct energy consumption levels associated with plant construction. Unfortunately, detailed data for these consumption levels are not available. This circumstance is to be discussed in greater detail in Section 6.1. Finally, the figure shows quite small MPRs for the aboveground (well-to-plant) piping and supports, which connect the plant to the wells.

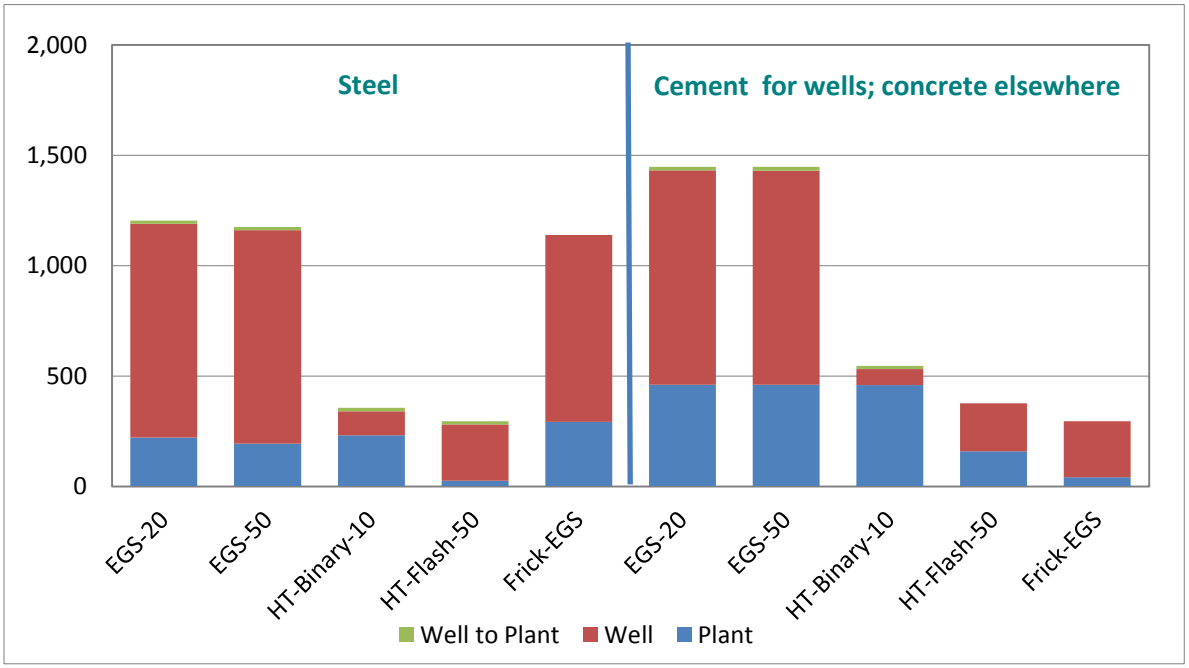

FIGURE 3 MPRs (tonnes/MW) for Geothermal Power Plants; Data from Table 2a

There are two additional sets of data in Table 2a that have been extracted from the literature. The analysis by Rule et al. (2009) evaluates a hydrothermal binary system in New Zealand, which is similar to Argonne's Scenario 3 (i.e., HT-Binary-10). Notice that the systems described by Rule et al. (2009) use more steel, concrete, and cement per MW than our hydrothermal binary, despite the fact that their wells are at a depth of 600 m relative to our wells at 1,500 meters. However, the likely reasons for the differences in material requirements are twofold: (1) Rule et al. (2009) assume a lifetime of 100 years as compared to our 30-year assumption, and (2) Rule et al. (2009) assume a well lifetime of 17 years, which results in considerably higher amounts of steel and cement required for drilling an additional 4 to 5 sets of new wells within their overall 100-year lifetime.

Another set of literature results (Frick et al. 2010) are also presented in the Table 2a and Figure 1. While the system evaluated by Frick et al. (2010) is an EGS binary plant like those in Argonne's Scenarios 1 and 2 (i.e., EGS-20 and EGS-50), their MPRs appear consistent with our values only for steel. Relative to our systems, the system described by Frick et al. (2010) apparently requires a considerably lower amount of concrete for plant buildings, less cement for their EGS wells, and approximately eight times the diesel fuel for well drilling. However, for well materials per meter drilled, they use 0.031 tonnes, 0.10 tonnes, and 213 L of cement, steel casing, and diesel, respectively. In our analysis, we estimate that 0.11 tonnes, 0.11 tonnes, and 43 L of cement, steel casing, and diesel fuel, respectively, are needed. Again, our use of steel casing is identical to theirs; factors contributing to observed differences could include well design, formation characteristics, and drilling equipment.

Our modeling demonstrated considerable variation associated with drilling wells and aboveground connection between wells and the plant. For wells, the variation can arise from different well depths, rock formation, source temperature, and other factors. For EGS systems drilled to 6 km, we find the coefficient of variation for cement, steel, and fuel to be around 55%, whereas it is closer to between 25% and 30% for the more shallow hydrothermal systems. Although they are a comparatively small contribution to mass-to-power ratios for the entire system, the coefficients of variation for the piping from plant to wells are: 40% to 50% for EGS and 25% to 30% for hydrothermal.

4 LCAs FOR THE OTHER POWER SYSTEMS

While our primary objective here is to establish the energy and carbon performance of geothermal power systems, it is important to compare their performance to those of other power generating systems. To that end, we employed materials and energy data extracted from the literature, using results exclusively from studies where infrastructure burdens have also been determined. A summary of these data including MPRs appear in Tables 2b and 2c. To facilitate comparisons of systems and the different studies within technologies, Figures 4–7 are also included. Our discussion starts with the conventional thermoelectric systems: coal, nuclear, and natural gas combined-cycle (NGCC). To give the reader a better sense of the level of use of the different electric power technologies, Table 6, extracted from GREET, depicts the average generation mix and technology shares for year 2010. The generation mix among the technologies are continually updated in GREET from data in the U.S. EIA's annual energy outlook (EIA 2010).

TABLE 6 GREET Default U.S. Generation Mix and Technology Shares (for year 2010)

	Residual Oil	NG	Coal	Biomass	Nuclear	Other Renewable[a]
Generation Mix	1.1%	20.2%	46.7%	0.7%	21%	10.3%
Technology Shares						
Utility Boiler	100%	20%	100%	100%		
Simple-Cycle Turbine		36%				
NGCC/IGCC[b]		44%	0%	0%		

[a] This category consists of hydro power, wind, geothermal, and solar, of which 6.9% is electricity from gravity hydro dams.
[b] IGCC = integrated gasification combined cycle.

4.1 COAL

Our assessment of coal focuses solely on conventional coal generation plants; integrated gasification combined cycle (IGCC) plants are not discussed because of the lack of current applications and studies. Although a typical coal-fired power plant has an output capacity of about 1,000 MW, coal plants in the United States can range from 10 MW to more than 2,000 MW. Coal plants are thermoelectric systems that burn coal to heat a boiler, which in turn generates steam that is directed through a turbine/generator set to produce electricity. The capacity factor for base load coal power plants ranges between 70% and 90%. The efficiency of these plants is around 34% on a low-heat basis, although the age and technology of a plant can affect this value a little. MPRs for the coal plants are given in Table 2b.

Pacca and Horvath (2002) conducted a comparative study of life cycle CO_2 emissions for a number of electricity-generating facilities, including hydroelectric, photovoltaic (PV), wind, coal, and natural gas combined-cycle plants. In the case of the coal plant, plant composition and construction data were obtained from an engineering firm that builds and designs power plants. Although the data collected represent a 1,000-MW plant, Pacca and Horvath (2002) scaled the

data to match that of a 913-MW facility for the purposes of performing the power plant comparisons presented in their paper. Their steel MPR includes the replacement of all boilers after 30 years of operation.

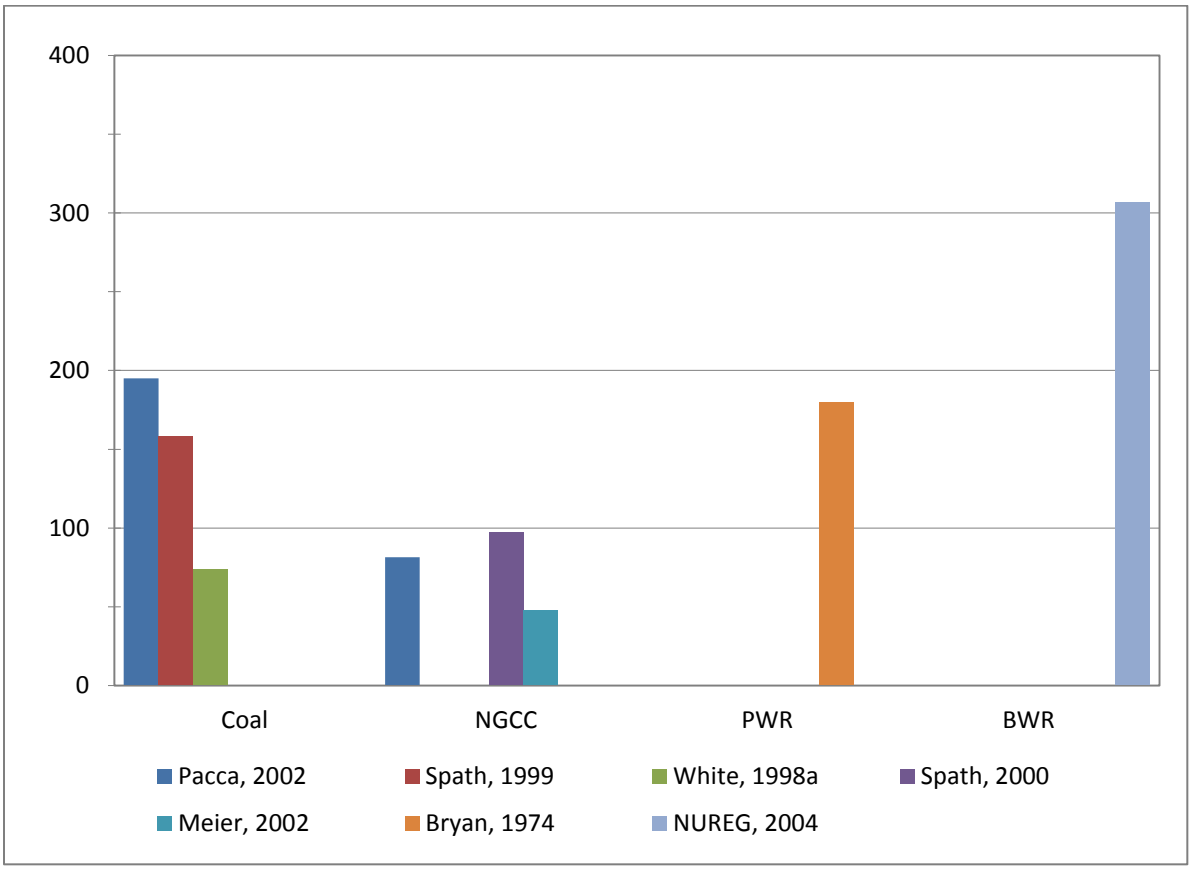

FIGURE 4 Concrete Content of Conventional Power Plants, tonnes/MW; Data from Table 2b

A second study that includes plant construction material data was conducted at the NREL by Spath et al. (1999). The goal of that study was to quantify and analyze the environmental implications of producing electricity from coal. The plant construction data (tonnes of various materials per MW of plant output) was derived from a DynaCorp (1995) report written under contracted with NREL. NREL also devoted effort to estimate rail, barge, and truck material requirements for mining and delivering coal to the plant. Although that data, provided (in parentheses) in Table 2b, are rightfully a part of the fuel cycle, they are not included in our estimates of energy and carbon metrics for the plant's infrastructure life cycle stage.

The final coal plant material entry considered in this analysis is from a study conducted at the University of Wisconsin to compare coal, wind, and nuclear electric power generation (White and Kulcinski 1998a). The purpose of that study was to compare the energy payback and carbon emissions associated with coal, wind, fission, and fusion power. The material data for the coal plant construction given in their report were obtained from an earlier national laboratory

report (El-Bassioni 1980). As seen in Table 2b, their material composition MPRs are considerably lower than are those from the other two studies. Based on the methodological approach employed by El-Bassioni (1980) of combining process-based with EIO LCA, it is possible that the materials embodied in equipment (e.g., turbine generator sets) housed in the plant might not have been included.

In summary, the materials used most often for coal plants by far are steel and concrete, followed by some use of aluminum. Other than steel, concrete, and aluminum, there is no total consistency across all of the studies on what materials to include. One study reported iron and another copper. However, because these materials appear in comparatively small quantities, they are not expected to significantly impact our energy and carbon results.

For the major MPRs given in Table 2b for coal (also see Figures 4 and 5 for steel and concrete), there is no conspicuous dependence on output capacity. A reduction in the normalized data might have been expected with increasing plant output capacity, although the range might be sufficiently narrow to expect such a trend to be evident. It is also of note that there is consistency in the relative amounts of steel, concrete, and aluminum from study to study. That is, the Pacca and Horvath (2002) study reports the largest amount of each material, White and Kulcinski (1998a) report the least, and Spath et al.'s (1999) estimates are in the middle. Hence, because of an absence of any apparent dependence of results on plant capacity, we must attribute the variation to other factors, such as data sources, data quality, and design variations. Because plant material composition data reported in the various studies were often obtained on an informal basis (e.g., personal communication) with little description of the methodology used for its acquisition, such data can be considered qualitative to semi-quantitative in part because of likely inconsistencies in how system boundaries were defined between studies. A second potential source of variation in the MPR results can be attributed to plant designs. In general, there are wide variations in plant designs for reasons that have to do both with desired plant designs and the peculiarities of a site. This factor was noted previously by Bryan (1974). Inter-study variation in MPR values can be expected because of some combination of limited data, system boundary differences, and the influence of design and plant location. However, it is not expected that such variations would obscure meaningful differences in materials composition metrics between generating technologies, especially if a few data sets are available for each.

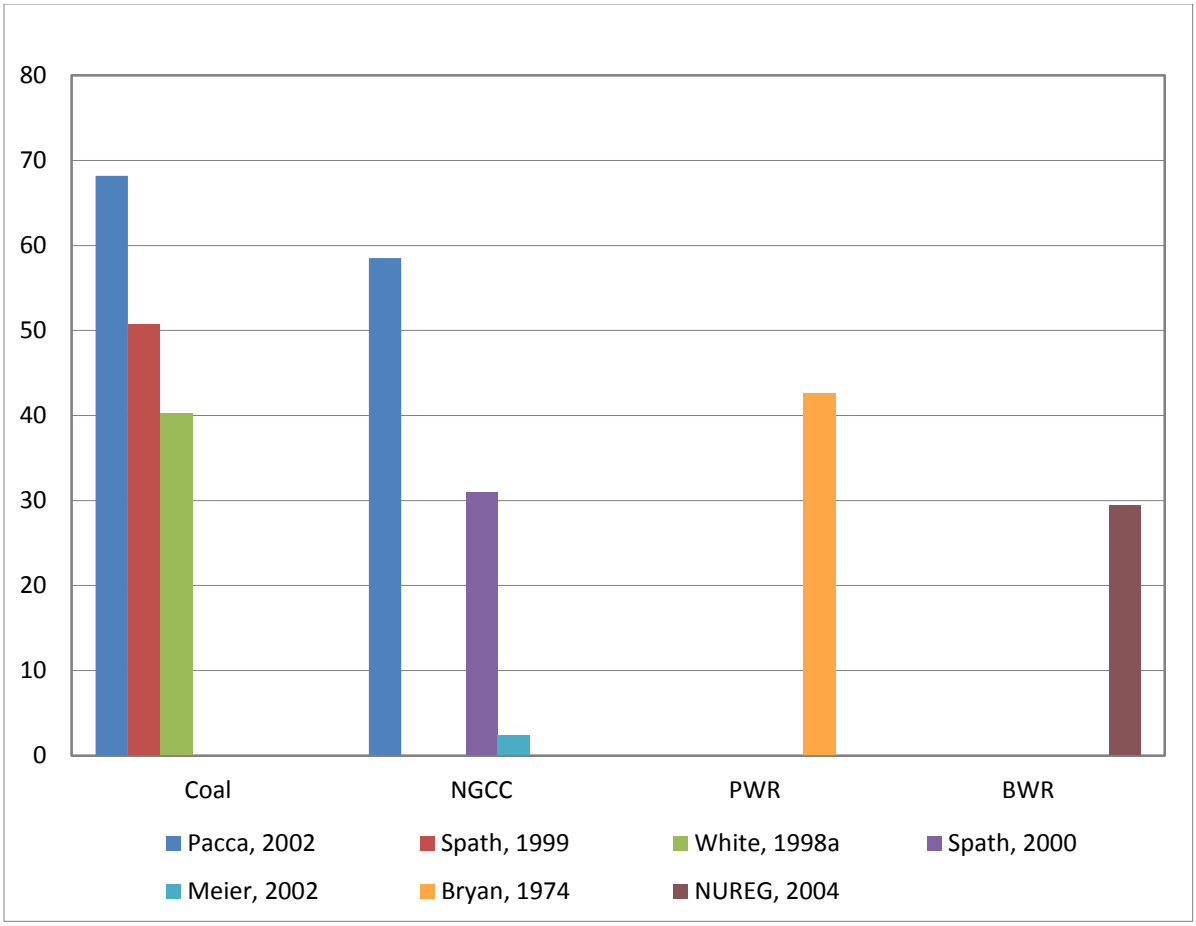

FIGURE 5 Steel Content of Conventional Power Plants, tonnes/MW; Data from Table 2b

4.2 NGCCs

For this analysis, we considered only combined cycle natural gas plants; gas-fired boiler technology was not covered because of the unavailability of studies containing composition and construction information. Furthermore, new gas-fired plants, which have come online in the past 20 or so years, are combined-cycle plants to serve primarily peak load power demand. Natural gas is a comparatively expensive fuel, and the combined-cycle plants, whether dual generator or combined heat and power, are more efficient and yield greater value per unit of input energy than do such plants as conventional coal-fired generation. The operating efficiencies for these types of plants can be as high as 53% on a lower heating value (LHV) basis.

We gathered data from three comparatively recent studies; see Table 2b and Figures 4 and 5 for details. The MPRs for Pacca and Horvath (2002) and Spath and Mann (2000) are comparable. However, the values from Meier (2002) are considerably lower than are the others, especially for the amount of steel and aluminum required. Because Meier's methodological approach is the same as White and Kulcinski's (1998a), a potential reason that the values are considerably lower might be that the equipment materials were not accounted for. Also given in Table 2b are the steel requirements for pipelines, which again have been added for the reader's

interest. Clearly, a considerable amount of steel is required for delivering the gas to the plant, a burden which should be attributed to the fuel cycle stage.

4.3 NUCLEAR POWER

A total of 104 nuclear electric plants are currently licensed by the U.S. Nuclear Regulatory Commission (NRC) and operating in the United States. Of these plants, 69 are pressurized water reactor (PWR) plants, and the other 35 are boiling water reactor (BWR) plants. Today, approximately 21% of U.S. electrical power comes from nuclear reactors. Current interest in reducing fossil carbon emissions may stimulate a new wave of nuclear power station construction projects. Power generation from both PWR and BWR plants is based on a steam cycle, and they typically operate at an efficiency (defined as energy in electricity vs. energy in steam) of around 32.5%. Normalized material composition data for a PWR and a BWR are given in Table 2b.

There is relatively little data available on the material composition of nuclear power plants. The most comprehensive data set available on plant material composition, published 35 years ago at Oakridge National Laboratory (Bryan and Dudley 1974), is for a PWR plant, and it is still frequently cited. It contains a very rich data set of plant material composition by plant systems (e.g., turbine generator, plant buildings, reactor equipment, condensing systems). Less comprehensive — but still useful — material composition data are available for a BWR plant from NUREG (2004). Because no new nuclear power plants have been built since the Three Mile Island incident, very little (if anything) has changed in plant material composition. Hence, the data extracted from the two cited references are certainly representative of plants in operation at this time within some range of variation.

As shown in Table 2b, the MPRs for these plants reveal some differences in material composition. According to the two data sets cited in the table, it appears that BWRs use about 3 times the amount of aluminum, two-thirds more concrete, about the same amount of copper, and about two-thirds the amount of steel of a PWR system. These differences likely occur because the higher-pressure vessel configurations of BWRs are less compact than are those of PWRs of comparable power.

4.4 HYDROELECTRIC

In the United States, about 6.9% of electricity is generated from hydroelectric facilities. The capacity factor for these plants is roughly 50%; see Table 2b for values. In this analysis, we include material composition data derived from three studies where hydroelectric generation was considered. The studies represent two gravity dams and one “run-of-the-river” facility. Pacca and Horvath (2002) considered the Glen Canyon dam facility, which is a gravity dam, and also included in their material assessment a plant upgrade to increase power output by approximately 39%. No estimate was provided on the likely lifetime of the facility. As the Glen Canyon dam is already 45 years old and the Hoover dam is even older, we assumed for the purposes of our

carbon dioxide calculation an effective lifetime of 100 years. The same lifetime assumption was used by Rule et al. (2009).

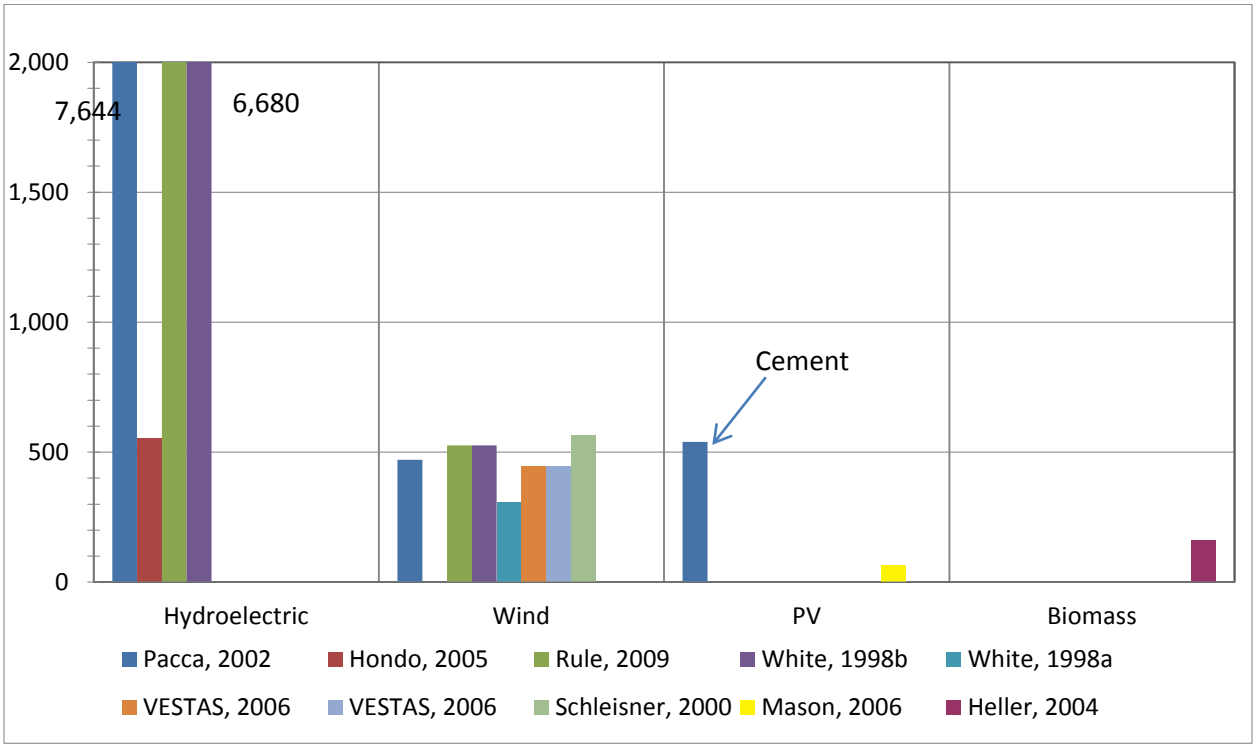

FIGURE 6 Concrete and Cement (when indicated) Use for Renewable Power Plants, tonnes/MW; Data from Tables 2b and 2c

We also include a hydroelectricity facility operating in New Zealand (Rule et al. 2009). From the supporting material accompanying their paper, we extracted material information for the plant and generated associated MPRs. The facility is the Clyde Dam on the Clutha River, the largest concrete gravity dam in New Zealand. The final set of metrics for our hydroelectricity assessment represents a facility operating in Japan (Hondo 2005). It is a "run-of-the-river" facility with a small dam. When compared to the other hydroelectric facilities given in the table, its power output is comparatively small. No useful information other than the concrete needed to build the facility can be extracted from the reference.

It is clear from Table 2b that the MPRs for the gravity dams are similar to one another. For steel and concrete (or cement), see Figures 6 and 7. Both facilities have large reservoirs (lakes) behind their dams, which is the primary reason for the very large concrete usage. The concrete MPR for the "run-of-the-river" plant is considerably smaller than those MPRs for the other two, which is to be expected for small dam facilities that holds back much less water. The Glen Canyon and Clyde dams are much higher (at 216.4 m and 106.1 m, respectively) than "run-of-the-river" dams, which are at most a few meters high and function to guide river flow into penstock piping.

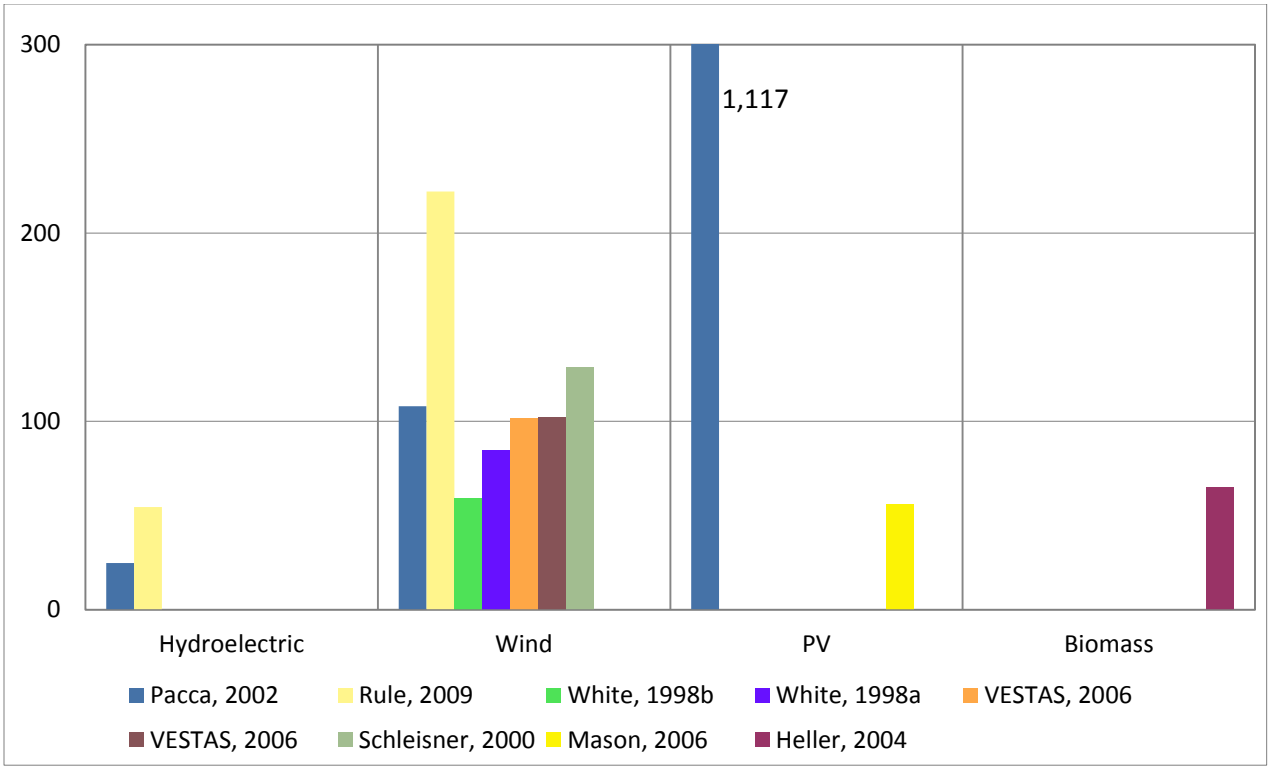

FIGURE 7 Steel Used for Renewable Power Plants, tonnes/MW

4.5 WIND POWER GENERATORS

Wind turbines are becoming increasingly popular in the United States and even more so in Europe. Denmark boasts that about 20% of its electricity comes from wind turbines. Currently, wind power supplies about 2.9% of U.S. electric power, but it is projected to grow to almost 4.1% by 2035 (EIA 2010). Wind generator capacities are becoming increasingly larger over time, and in terms of power output, today's ranges are between 1 to 3 MW per turbine.

MPR values from the reviewed wind power life cycle studies appear in Table 2c. For concrete and steel uses, also see Figures 6 and 7. An inspection of the table reveals relatively consistent uses of steel, where the minimum and maximum values range in difference by about a factor of four. The lowest value is from White and Kulcinski (1998a). However, as noted above, material composition values published by White and Kulcinski (1998a) and Meier (2002) tend to be consistently lower than other studies. The highest values reported here are from Rule et al. (2009). The reason for this finding is not clear, although it might be related to the wind farm's 100-year lifetime and associated replacements for generators and other assets. A reasonably well-documented LCA published by Vestas (2006) has the most comprehensive material listing of the studies cited. Two sets of their results are cited; one for a single generator, and the other for a 182-turbine wind farm and including grid connection assets. The hypothetical wind farm by Pacca and Horvath (2002) is sited in Southern Utah and those by White and Kulcinski (1998a, 1998b) correspond to the Buffalo Ridge wind farm (Minnesota).

There appears to be greater consistency of concrete use among the studies. The range for concrete is about a factor of two. Compared to the conventional power generating facilities, there is a substantial amount of fiberglass and plastic on wind turbines. These materials are in the nacelle cover for a wind turbine, which is a glass fiber reinforced epoxy material (a plastic).

4.6 PHOTOVOLTAIC POWER

Photovoltaic power currently provides a very small fraction of a percent of today's total electric power, and EIA projects that it will still be only about 0.01% of total generation by 2035 (EIA 2010).

The material composition of PV arrays is distinctly different from the other forms of electric power generation. PV arrays, like wind turbines, contain considerable amounts of glass and polymer. There are also significant amounts of aluminum and silicon; production of both of these materials is very energy intensive. Glass is used as a transparent cover of the photo array assemblies, and the polymer (polyethylvinylacetate) is used to encapsulate the silicon arrays, which are the heart of the assemblies, protecting them from the weather and environment. The back cover for the assemblies consists of layers of polymer and aluminum.

MPRs for PV arrays from four different studies have been included in Table 2c and Figures 6 and 7 for steel and cement. Pacca and Horvath (2002) reported high values for the MPRs for all materials, especially steel. The reason for their high values is unknown. The MPRs from Mason et al. (2006) are more moderate for cement, steel, copper, and aluminum. Neither of these studies report any glass or silicon use, two very important components of PV systems. On the other hand, the studies of Phylipsen et al. (1995) and de Wild-Schoulten and Alsema (2005) list copper, silicon, glass, and polymer uses in PV arrays, although no listings of steel and cement are included. Hence, the latter two studies do not appear to formally consider array deployment and installation.

4.7 BIOMASS POWER

At present, around 0.7% of U.S. electricity generation comes from combustion of biomass (e.g., forestry residue, energy crops, municipal solid waste), and it is expected to grow to 2.9% by 2035 (EIA 2010). We were unable to find any life cycle assessment studies of conventional biomass power plants that included plant infrastructure data. One study addressed a biomass gasification-to-electricity plant (Mann and Spath 1997); however, as no such facility is in operation at this time, it is not included herein. Instead, we have combined results of two studies to represent a conventional thermoelectric biomass-to-electricity plant. Because biomass-to-electricity plants are thermoelectric systems, we employ coal plant data (Spath et al. 1999) for the material requirements as a suitable surrogate representation. Having based our material requirements on large coal plants, we recognize that our estimated MPRs for the biomass plant with a comparatively low power capacity may be underestimated somewhat, as larger plants need less material per MW output than do smaller ones. For the purposes of this study, we believe this approach provides a reasonable approximation. For the material composition needs

of the additional equipment used for biomass preparation, material data from Heller et al. (2004) were used. MPRs are given in Table 2c. Henceforth, our modeled biomass direct-fired boiler power system is denoted Biomass-88, for an 88-MW plant.

As seen in Tables 2b and 2c and Figures 4 through 7, the MPRs for the biomass plant are very similar to those used for coal and nuclear plants. This result is not surprising given the use of coal plant material composition data. Nevertheless, the additional material for the biomass material handling system at the plant did not substantially change the overall infrastructure material composition of the plant. In Table 2c, we included the steel associated with the trucks required to deliver the biomass feed to the plant in parenthesis, as this material belongs to the fuel production stage of the plant's life cycle. This value is higher than that reported for a conventional coal plant. The likely reason for this result is the lower specific energy and density of the fuel feedstock.

Another way to look at plant material composition is the total mass of all materials per unit power output. This is shown in Figure 8. It is clear from the figure that conventional power technologies require considerably lower masses of constituent materials than do most of the renewable technologies. Biomass-based electricity is relatively low in material requirements per

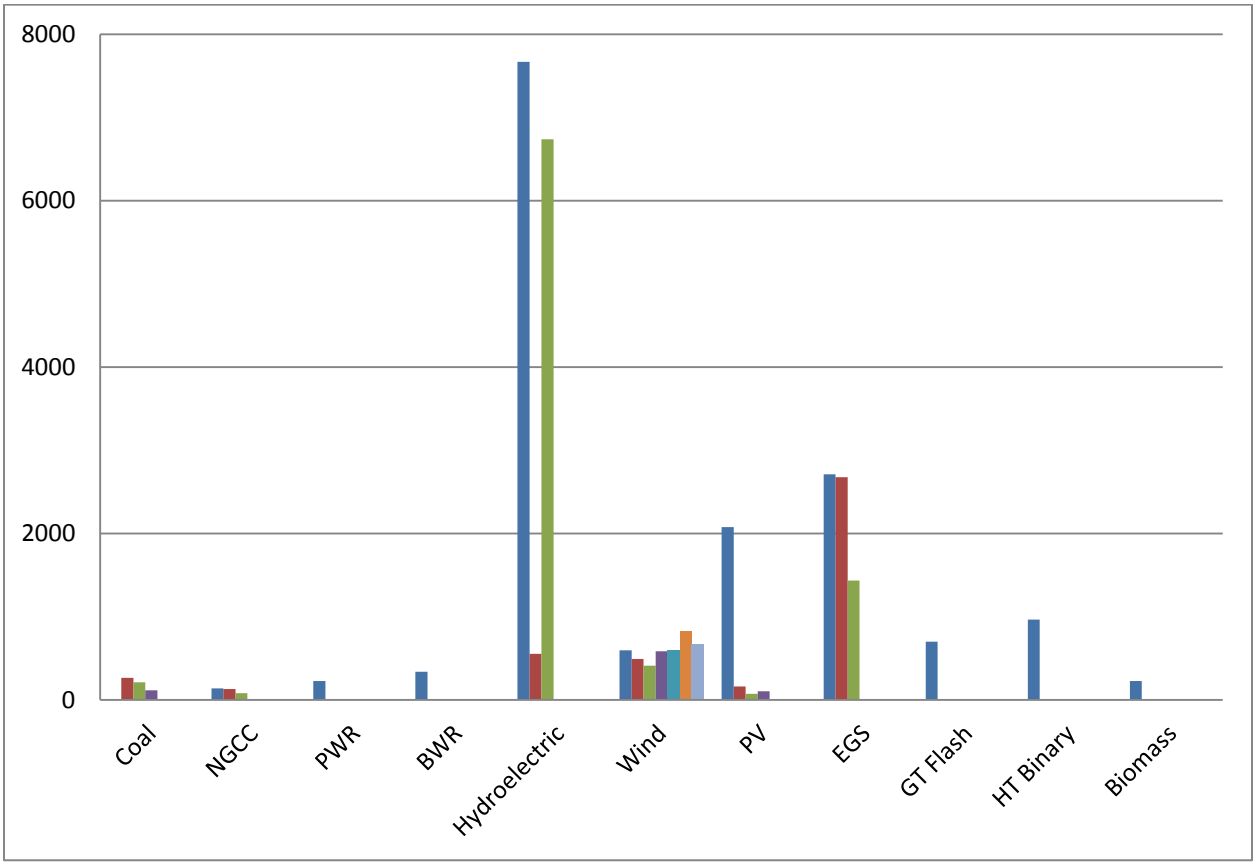

FIGURE 8 Total Compositional Mass (tonnes/MW) for Various Power-Generating Technologies (see Tables 2a–2c for individual values)

unit of power output. Of the four studies reviewed for PV, there is significant variation in materials per unit of power. Of the remaining renewable power technologies, gravity dam hydroelectric is the highest, followed by EGS geothermal, hydrothermal binary and flash, and lastly by wind.

4.8 PLANT MATERIAL SUMMARY

On the basis of the MPR results above, it is found that the amounts of materials like steel and concrete required to build and equip a power plant are the lowest for the conventional power systems (i.e., thermoelectric systems, including coal, natural gas combined cycle, and nuclear). Biomass-to-power, a thermoelectric renewable system, shows the same material dependence. Other materials, like copper and aluminum, were tracked but their use is considerably lower for these power systems. Renewable systems generally require more steel and concrete per MW of capacity than conventional systems require, especially for EGS and wind. In the case of EGS and hydrothermal binary plants, this result is attributed to the deeper wells and air-cooled condenser systems needed for the binary plants. Temperature of the resource also plays an important role in this case; a lower-temperature resource, typical of an EGS, requires greater fluid flow and hence needs to have more wells built and in operation to attain a given power output. A considerable amount of aluminum is needed for EGSs, as this material is important for the heat-exchanging function in the air cooled condensers. Hydroelectric gravity dams require the most concrete. Concrete requirements appear to be quite variable for photovoltaic systems, which, on the other hand, require about the same amount of aluminum as EGS and hydrothermal binary systems. Aluminum is used for the photo array frames.

5 DESCRIPTION OF THE EXPANSION OF POWER GENERATION SIMULATIONS IN GREET

To evaluate the life-cycle energy consumption and GHG emissions for various types of electricity generation, the analysis in this study considered the extraction, production, and transportation of all fuels required (including electricity) to construct the plant; to produce plant constituent materials, including those used in equipment and to power the plant; and finally, to decommission the plant (see Figure 1). The fuel- and plant-cycle analyses are conducted by using the Argonne GREET model (Wang 1999). This model is known as GREET 1. GREET 2 has recently been extended to address the full life cycle of vehicles (Burnham et al. 2006) and now includes the life cycle stages of material production, parts manufacturing and vehicle assembly, maintenance and repair, and vehicle end-of-life management. The GREET family of models is being extended once again to include the life cycle of electricity generation and the facilities that provide that product (i.e., power).

5.1 FUEL CYCLE

Well-to-plant (WTP) stage data, which cover the extraction, production, and transportation of fuel to the end-use site, are used for this analysis. Fuel use data are also employed. The default assumptions in GREET 1, developed for the fuel-cycle analysis, are applied, except for the use of forest residue as a biomass power plant's feedstock. The GREET models track all carbon emissions associated with a fuel, even if it is derived from the biosphere. In such cases, that carbon is subtracted out later in the analysis as a carbon credit, a practice that recognizes the cyclic nature of carbon moving between the biosphere and technosphere.

In this study, forest residue is considered to be carbon neutral on a global basis. This treatment assumes that the newly available forest residue globally compensates for the newly burned forest residue in power plants within a given (and short) time period.

5.2 PLANT CYCLE

For the plant-cycle analysis including the recovery, production, and end use of construction materials, GREET 2, developed for the vehicle-cycle analysis, was expanded by adding new material pathways and plant-construction data. The plant-cycle energy uses and emissions are estimated by multiplying the fuels and materials required in plant construction with the upstream energy uses and emissions for fuel and material production. The fuel and material requirements per energy output are obtained from the requirements per generation capacity in Tables 2a–2c by dividing them with the utility factor (the ratio of the actual generation to the generation capacity) and the lifetime of power plants.

The upstream energy uses, emissions for fuel production, emissions for materials production, and the on-site fuel consumption are obtained from GREET 1 by using GREET's default assumptions. The assumptions include the U.S. average generation mix and the

U.S. conventional diesel and natural gas recovered in North America. The emission factors for diesel-fired and natural gas-fired commercial boilers are used to estimate the emissions for on-site diesel and natural gas combustion, respectively. The upstream energy uses and emissions for most materials, such as aluminum, copper, iron, and glass, are obtained from GREET 2. Other materials are defined differently and include steel, cement, concrete, and silicon. For example, because steel associated with construction is primarily produced by using the electric arc furnace (EAF), we use GREET's EAF data for steel production. In addition, GREET's assumptions for sheet production and rolling are used to approximate the production process of steel products for construction (e.g., for I-beam and pipes). For the pathways that are not available in GREET 2, this study relies on cradle-to-gate (CTG) energy uses from other studies (e.g., U.S. LCI Database). The CTG energy uses are often provided as aggregated information for material production while GREET models each process separately (such as mining and refining) and combines them to obtain the life-cycle energy uses and emissions. Table 7 summarizes the energy uses and the shares of process fuels for important material production in power plant infrastructure, as well as total GHG emissions. Note that the total energy and emissions includes both direct and indirect energy uses and emissions.

CTG results of cement are based on an LCI database value for Portland cement (U.S. LCI Database undated). The cement production process generates significant emissions of CO_2. The CO_2eq emissions associated with process fuels are 1.07 kg CO_2eq/kg cement. Calcining limestone, basically $CaCO_3$, to lime (CaO) liberates 0.51 kg of CO_2 per kg of cement in the process. We assume that concrete consists of 21% of cement, 41% of aggregates, 29% of sand, and 9% of water (Kendall 2007). Assuming that the aggregates, sand, and water have no or negligible CTG energy uses and emissions, CTG energy uses and emissions for concrete are 21% of those for cement. For silicon, the process data from the literature (de Wild-Schoulten and Alsema 2005) are used. Only 37% of the silicon used to make a solar array is actually incorporated into the unit; the rest is discarded as scrap, with the majority of it being associated with wafer sawing. Hence, for reasons of production efficiency, the silicon, despite the small amounts of it that are used, still makes an appreciable contribution to the energy and carbon burdens of a PV array (3,740 MJ/kg of silicon and 297 kg of CO_2 eq/kg of silicon).

PV facilities, unlike other power plants, require significant amounts of materials, such as aluminum and glass. Therefore, the dominant energy and carbon-intensive materials for PV plants, which use little concrete and steel, are silicon, aluminum, and glass. Steel and concrete, however, are widely used in all of the other power plants. Therefore, based on the energy- and carbon-intensity levels, steel is generally expected to be the most significant material in the power plant LCAs, followed by concrete for those systems.

The final stage of the plant cycle or end-of-life (EOL) stage is plant decommissioning and the recycling of recovered materials. Decommissioning and recycling are not considered here for two reasons: (1) there is a general lack of available data, and (2) its magnitude is small. In fact, Meier's (2002) analysis of the life cycle of an NGCC plant showed that the energy and GHG emissions for the EOL stage are just a few percentage points of the plant cycle, which, in turn, is a small fraction of total plant life-cycle results.

TABLE 7 Energy Uses for Material Production

Material	Iron[a]		Aluminum[a]			
Process	Recycling	Casting	Mining	Refining	Alumina Reduction	Melting and Casting
Energy Use: MJ/kg	1.6	24.0	3.1	21.1	76.6	4.8
Shares of Process Fuels (%)						
Residual Oil	0.0	0.0	0.0	0.3	17.2	2.8
Diesel	93.0	0.0	100.0	0.0	0.0	0.0
Natural Gas	0.0	0.0	0.0	89.4	4.6	91.7
Coal	0.0	0.0	0.0	3.7	5.9	0.0
Electricity	7.0	100.0	0.0	6.6	72.3	5.5
Total Energy: MJ/kg	2.0	30.7	3.7	24.6	120.6	5.6
Total GHGs: kg CO_2e/kg	0.15	0.38	0.29	1.63	7.83	0.36

Material	Steel[a]		Copper[a]	Silicon[b]	Cement[c]	Concrete[c]
Process	EAF	Production	Production	Production	Production	Production
Energy Use: MJ/kg	4.9	7.1	76.7	1792.3	4.8	1.0
Shares of Process Fuels (%)						
Residual Oil	0.0	0.0	36.4	0.0	0.0	0.0
Diesel	0.0	0.0	0.0	0.0	0.9	0.9
Natural Gas	5.4	84.4	39.6	28.3	4.4	4.4
Coal	0.0	0.0	0.0	3.3	58.8	58.8
Electricity	94.6	15.6	24.0	68.4	10.8	10.8
Pet Coke					16.3	16.3
Other					8.7	8.7
Non-combustion CO_2: kg/kg					0.51	0.11
Total Energy: MJ/kg	8.3	9.3	111.3	3,747.1	6.4	1.3
Total GHGs: kg CO_2e/kg	0.46	0.63	8.48	296.69	1.58	0.33

[a] GREET; [b] de Wild-Schoulten and Alsema (2005); [c] U.S. LCI Database (undated).

6 RESULTS AND DISCUSSION

In order to compare the environmental performance of the electricity-generating technologies discussed herein and the impact of facility construction, we compute a pair of energy and CO_2-equivalent GHG emissions metrics. They are E_{pc}/E_{out} (Figure 9) and GHG_{pc}/E_{out}, (Figure 10) and are based on a per-unit energy output basis (the service functional unit). For notational simplicity, they are henceforth denoted as the energy ratio and specific carbon, $\mathcal{E}_{pc}$ and GHG_{pc}, respectively. The former is dimensionless, and the later has units of gCO_2eq/kWh. Note that the GREET model's GHG output is a complete greenhouse gas estimate, while some authors cited herein report only CO_2 emissions. Generally, the difference is a few percentage points.

6.1 CONSISTENCY BETWEEN GREET AND PUBLISHED RESULTS

Our first task is to establish the consistency of our $\mathcal{E}_{pc}$ and GHG_{pc} results in comparison to those published in the references, from which our materials data were taken. To facilitate the comparison, we present results found in Figures A1 through A6 of the Appendix. From an inspection of the figures, it is clear that, on balance, the GREET $\mathcal{E}_{pc}$ and GHGinf results are somewhat lower than values computed in the corresponding references. This finding is consistently so when compared to the work of Meier (2002), White and Kulcinski (1998a), Rule et al. (2009), and Schleisner (2000). The reason for these differences is that these authors used higher production energy values for steel than are employed here. Because EAFs are typically used for making "long product," which is characteristic of most of the steel used for construction and equipment applications, the GREET value for EAF steel was employed for our study. Because of the use of recycled steel as a feedstock, the production energy for steel from an EAF is lower than that from a basic oxygen furnace, which obtains most of its feed from a blast furnace. Considering the differences in steel production energies, the GREET $\mathcal{E}_{pc}$ and GHG_{pc} results and those from the authors just mentioned are in reasonably good accord.

The $\mathcal{E}_{pc}$ and GHG_{pc} values extracted from Hondo (2005), Meier (2002), and White and Kulcinski (1998a) were determined by process-based LCA; the additional results found in those references were derived by using input/output analysis. For example, from White and Kulcinski's (1998a) report, an infrastructure energy ratio for coal is estimated to be 0.0046, which is the sum of 0.0017 computed from plant materials using process LCA methods and 0.0029 for plant construction operations estimated using the EIO method. Our value for $\mathcal{E}_{pc}$ is 0.0011, which is in reasonable accord with White and Kulcinski's value of 0.0017. The rationale for not using the EIO approach or results herein was discussed in the methods section (Section 2).

Whether from the references or geothermal model results, the GREET model uses data on: (1) plant material composition, (2) equipment material composition, (3) equipment production, and (4) construction site fuel and power requirements. From these data and production energy data for materials found in GREET, values for $\mathcal{E}$pc and GHGpc are computed. Unfortunately, data for items 3 and 4 are generally unavailable; in fact, it is even unclear whether plant material composition data cited in the references includes the materials comprising plant

equipment (e.g., turbines, generators, condensers). However, some studies have apparently had access to type 3 and 4 information, for example, the two NREL studies shown in Figure A4 (Spath et al. 1999; Spath and Mann 2000). In fact, the GHG_{pc} values extracted from those references are around 4 to 6 times the values calculated from GREET when using the references' respective plant material composition data. Otherwise, Figure A4 shows that GHG_{pc} is quite consistent across the coal, natural gas, and nuclear technologies. In fact, the NREL studies did account for plant decommissioning and fuels for transporting equipment and materials and for construction. Unfortunately, other than for plant composition, specific details about these other inputs are not provided in those reports. This lack of detail, however, may indicate that those inputs are an implicit part of the life cycle packages used to compute their published results.

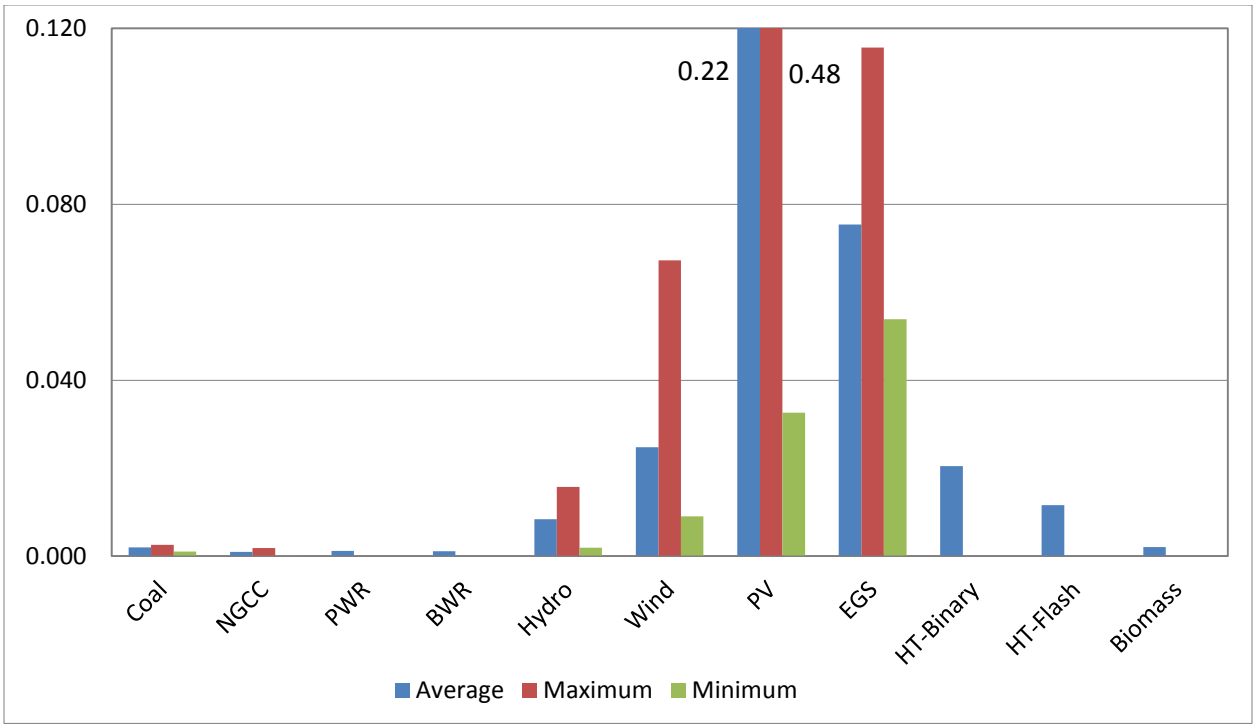

FIGURE 9 E_{pc}/E_{out} Values for the Power-Generating Technologies Covered as Determined from GREET

In conclusion, GREET-based estimates of $\mathcal{E}_{pc}$ and GHG_{pc} are generally in reasonable agreement with literature values, especially when differences can be attributed to variations in production energy for system-constituent materials. But when studies have included data from activities not available for inclusion into GREET, such as fuel used during construction, substantial differences exist between GREET-based estimate $\mathcal{E}_{pc}$ and GHG_{pc} and those from the corresponding literature.

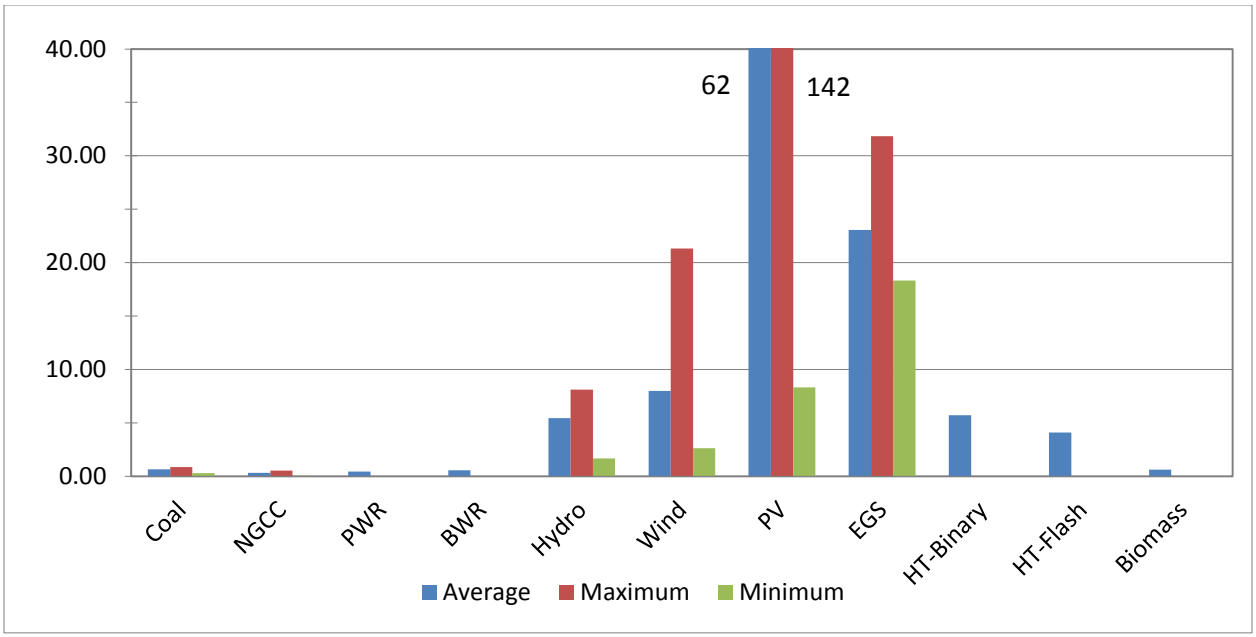

FIGURE 10 GHG_{pc}/E_{out} in g of CO_2eq per kWh for the Power-Generation Technologies Addressed as Determined from GREET

6.2 COMPARISON OF $\mathcal{E}_{pc}$ AND GHG_{pc} VALUES FOR THE POWER-GENERATING TECHNOLOGIES

Based on the material composition and plant performance data found in Tables 2a, 2b, and 2c and on the life cycle energy and GHG data for fuels and materials found in GREET, values of $\mathcal{E}_{pc}$ and GHG_{pc} were estimated for the electricity-generating technologies covered herein. Those results are presented in Table A1. To facilitate an easier comparison of results, Figures 9 and 10 are included. For the purpose of establishing the relative magnitude of GHGpc compared to GHGs from other life cycle stages, normalized GHG values have also been included in Table A1for the fuel production and fuel use stages of the electricity life cycle. Finally, Table A1 and Figures 9 and 10 also include range information (maximum and minimum values) for $\mathcal{E}_{pc}$ and GHG_{pc}.

An inspection of these two figures and Table A1 reveals some important trends. First, $\mathcal{E}_{pc}$ ranges between 0.001 to 0.003 for almost all of the thermoelectric technologies (i.e., coal, NGCC, nuclear, and biomass). However, the geothermal systems appear to be exceptions. $\mathcal{E}_{pc}$ for the enhanced geothermal binary system (EGS) is about six times that of the flash plant, which, in turn, is about 5 times that of the other thermoelectric plants. For the flash plant alone, excluding the steel and cement associated with the well field and the aboveground piping between the field and the plant, $\mathcal{E}_{pc}$ and GHG_{pc} are found to be 0.001 and 0.30, respectively. These values are similar to the values for the other thermoelectric facilities provided in the table and as such, when compared to the overall system, show the significance of the extra energy and carbon burdens associated with wells and well-to-plant connections for geothermal systems. On the other hand, the $\mathcal{E}_{pc}$ and GHG_{pc} values for the EGS system are considerably larger than are those of the geothermal flash plants. There are two reasons for this result: (1) a very large air-cooling

structure required for the binary plant condenser comprises about half of the plant's steel and concrete; and (2) very large amounts of cement, steel, and fuel are needed for developing a deep 6-km well field. Notice that the carbon and energy metrics for the hydrothermal binary plant are intermediate to those of EGS and flash technologies. This result is as expected. The hydrothermal binary system has increased hardware and equipment requirements than does a flash plant, but at the same time, its wells are more shallow than those used in the EGS technology.

For our EGS analysis, we are taking the conservative approach and assume the well depth to be 6 km, which was the upper limit of the EGS scenarios. However, because some EGS wells are certain to be more shallow, we present additional results assuming 4-km wells. Aboveground plant-to-well connections remain unchanged. Along with the 6-km results, additional 4 km-based results are included in Table 8. It is clear from the table that well depth significantly impacts $\mathcal{E}_{pc}$ and GHG_{pc}; both decrease by about a factor of two in going from 4- to 6-km well depths.

TABLE 8 Energy Ratio and Specific Carbon for EGS with Different Well Depths

System	E_{pc}	GHG_{pc}
EGS 20: 6 km	0.052	18.9
EGS 20: 4 km	0.029	8.5
EGS 50: 6 km	0.054	18.3
EGS 50: 4 km	0.026	8.4

Another trend evident in Figure 9 is that $\mathcal{E}_{pc}$ exceeds 1% for almost all of the renewable power-generating technologies. This finding is especially true for PV systems and EGS. The average value reported in the figure for PV systems is consistent with a previous assessment (Keoleian and Lewis 2003), indicating that around 25% of an array's lifetime is devoted to energy payback. Regarding the range of results shown in the figure for photovoltaic systems, the Pacca and Horvath (2002) results seem too high. Taken at face value, their energy ratio implies that almost half of the system's output is needed for energy payback. However, if one considers the primary energy displaced by using PV versus electric power generated conventionally, the ratio is considerably lower. The average value for PV reported in the table is very close to de Wild-Schoulten and Alsema (2005) results, which are probably the most detailed LCA information for polycrystalline and single crystalline silicon PV arrays published to date.

With the exception of PV and EGS, the $\mathcal{E}_{pc}$ values shown in Figure 9 range from between one-tenth of a percent and a few percentage points for the energy technologies discussed herein. This result is consistent with other studies that have explored the magnitude of "capital energy," (i.e., in this case, the energy for the plant cycle). Boustead and Hancock (1979) report that for most production facilities, whether power plants or factories, the energy required to produce all of the constituent elements of facilities and their subsequent construction is on the order of a few percentage points of the energy required to produce and use the products manufactured over the lifetime of the plant.

6.3 COMPARISON OF ENERGY CONSUMPTION AND GHG EMISSIONS AMONG TECHNOLOGIES

Figures 11–15 provide information to help compare $\mathcal{E}_{pc}$ and GHG_{pc} among technologies. Values shown in the figures represent averages of results compiled herein for each power-generating technology. To compare the various power-generating technologies in a meaningful way, a consistent basis of comparison is needed. Using total energy input is one possibility. Thus, by using the total energy required to produce a kWh of electrical energy over the life cycle of a power plant as a basis, Figure 11 shows that more energy is being consumed than is delivered to the consumer. This result is, of course, expected as no commercial process is perfectly efficient. The energy levels per kWh shown in this figure are generally from different sources, such as fossil, biomass, and nuclear. Although figures such as this remind us that energy is not free, it is nonetheless misleading. In fact, because of procedural conventions, the methods for accounting for these energies per kWh are not consistent. For example, the coal energy is based (quite reasonably) on the energy content of the coal plus other energy consumption amounts related fuel production and plant cycle, whereas for hydroelectric generation, there is apparently no accounting for the gravitational energy potential of falling water, from which the delivered power is derived. And where is the accounting for the sunlight that powers PV systems? The biomass power bar accounts for the energy content of the biomass plus fuel production and plant cycle consumptions. On the other hand, the thermal energy of geofluids is not included in the figure.

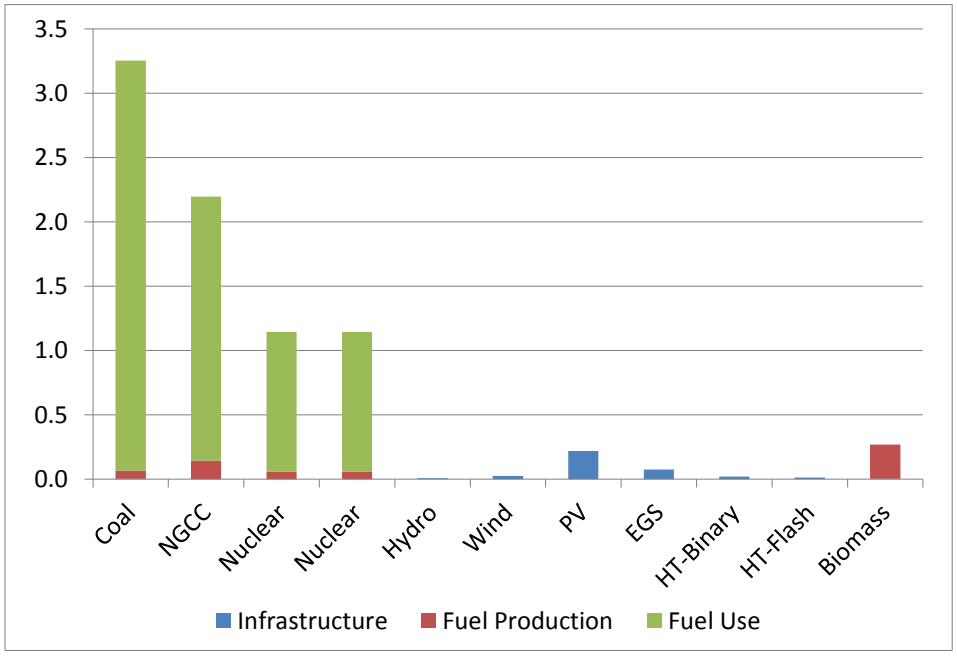

FIGURE 11 Total Energy Consumption (kWh) per kWh Output for Different Power-Generating Technologies as Determined from GREET

A more consistent way to view energy consumption in power production is to base it on a factor that is a significant motivation for diversifying power generation. Because reduction of fossil energy use is just such a motive, a graphic showing the fossil energy requirement per kWh output is a useful basis of comparison for the different generating technologies (Figure 12).

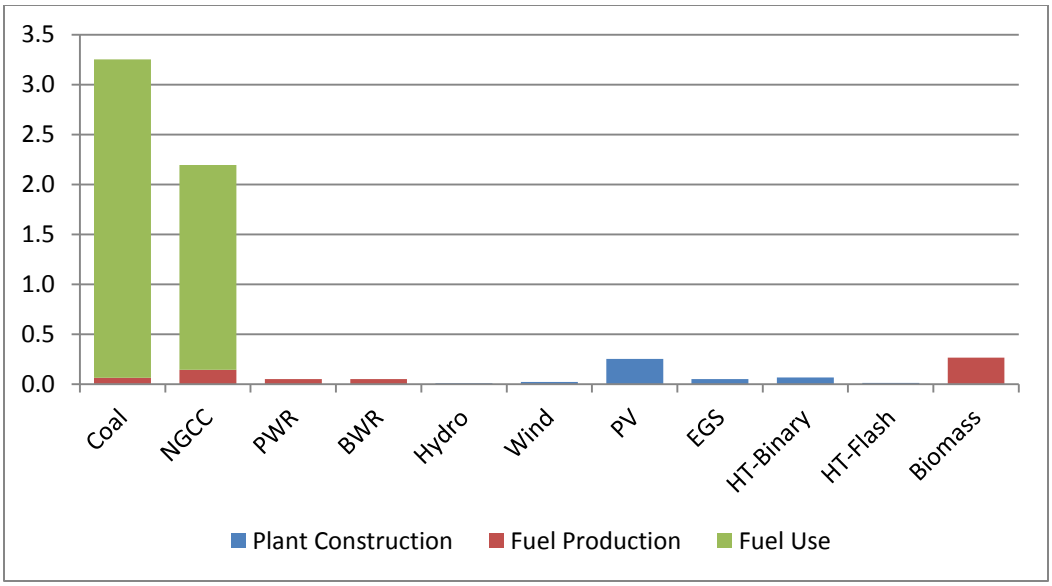

FIGURE 12 Fossil Energy Consumption (kWh) per kWh Output for Different Power-Generating Technologies as Determined in GREET

It is clear from the figure that all of the generating technologies use some fossil energy. (Fossil energy uses for wind and hydroelectric power plants are not zero; they are small and therefore do not register on the graph.) Not surprisingly, the fossil fuel plants use considerably larger amounts of fossil fuels than do any of the other generating technologies. Incidentally, an important capability of the GREET model is to itemize the components (coal, natural gas, oil) of the fossil energy requirements shown in Figure 11 (see Figures 13–15).

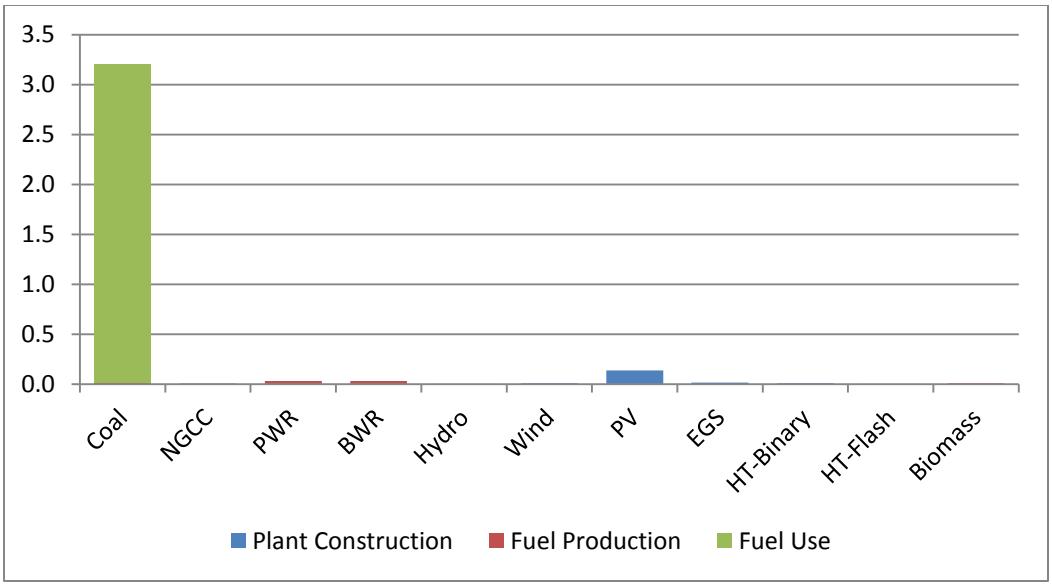

FIGURE 13 Coal Energy Requirements (kWh) per kWh Output for the Various Power-Generating Technologies as Determined in GREET

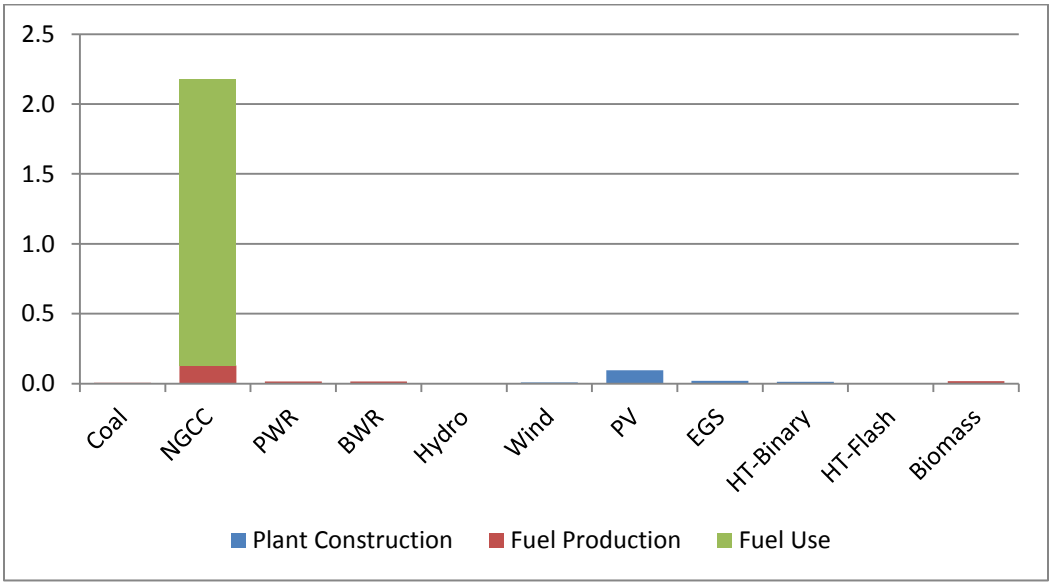

FIGURE 14 Natural Gas Energy Requirements (kWh) per kWh Output for the Various Power-Generating Technologies as Determined in GREET

As seen in Figure 13, not only is the expected dependence of coal-based power generation on coal consumption a conspicuous result, but coal is also required for PV and nuclear generation. In those cases, coal-based electricity is employed in both the production of materials needed for PV plants and for processing the uranium fuel needed for nuclear plants.

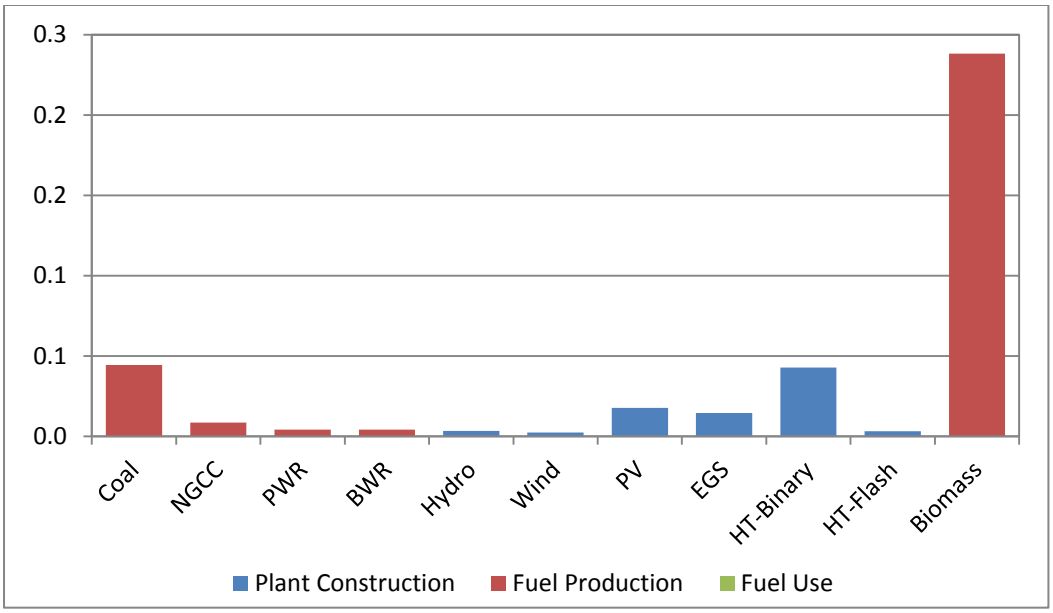

FIGURE 15 Petroleum Energy Requirements (kWh) per kWh Output for the Various Power-Generating Technologies as Determined in GREET

An inspection of Figure 14 shows the expected dependence of NG-based electricity on natural gas energy not only for fuel use but also for fuel production. This figure also shows natural gas requirements for material production in PV and EGS systems, more specifically for the production aluminum frames and silicon for PV systems and aluminum heat-exchanger fins for EGS. And finally, Figure 15 shows the petroleum energy requirements for the various power-generating technologies. For the thermoelectric systems, diesel and gasoline fuels are required during fuel production to transport fuels to the site of use. Notice that the value is highest for biomass-based electricity. This result is attributable to collecting and transporting biomass feeds, which are forest residues, a comparatively low-energy-density fuel. Finally, some petroleum energy is required during the infrastructure stage for PV, hydroelectric, EGS, wind, and hydrothermal binary and flash power technologies. With the exception of geothermal systems, petroleum uses seen in Figure 15 are associated with material production during the plant cycle stage. On the other hand, in the case of geothermal systems, the petroleum consumption during the plant cycle stage is primarily attributable to the diesel fuel required for drilling wells. Because values in the figure are averages, petroleum consumption associated with hydrothermal binary power production is seen to be higher than its EGS counterpart because of a very high diesel demand for well drilling cited in one of the references (Frick et al. 2010).

As a result of current concerns over climate change, it is both useful and relevant to compare GHG emissions for the different power generating technologies. Toward that end, Figure 16 shows the GHG emissions per kWh delivered over the life cycles of the power-generating technologies studied.

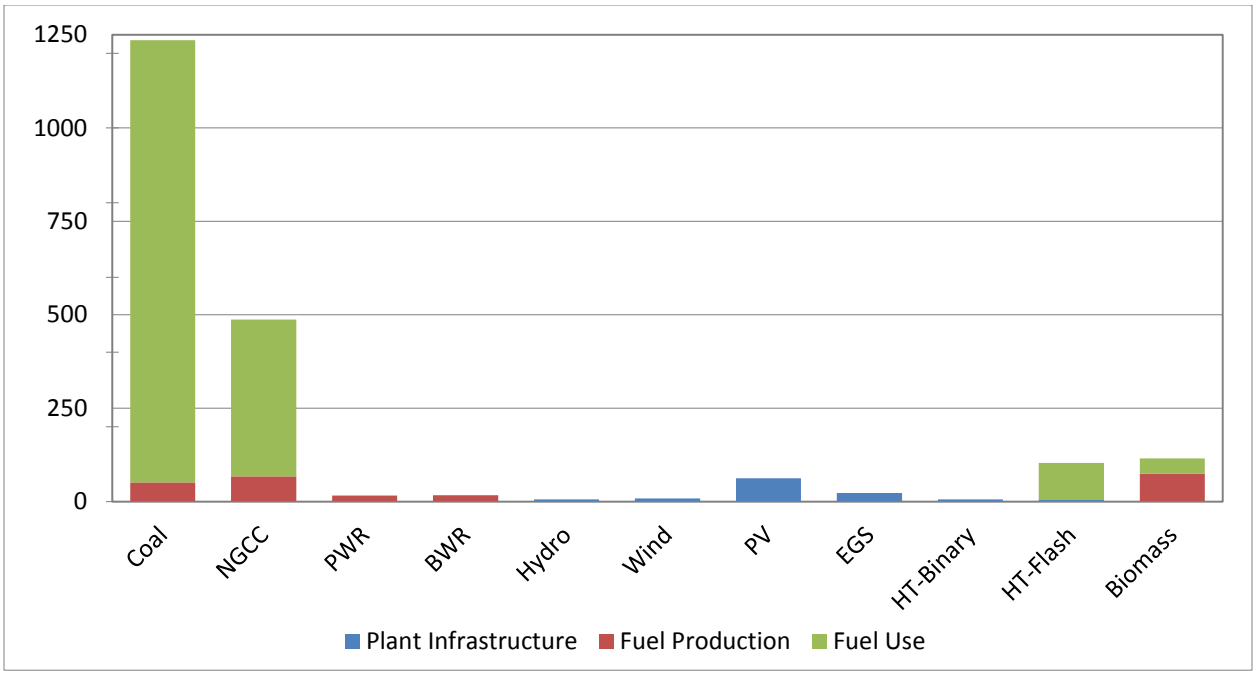

FIGURE 16 GHG Emissions (gCO_2e/kWh) by Life Cycle Stage for Various Power-Generating Technologies as Determined in GREET 2.7

First, notice that Figures 12 and 16 are virtual mirror images of one another. As is evident from the "total" GHG plots shown in Figure 16, all electric power-generating technologies have at least some GHG emissions, although the amounts are quite variable in magnitude. Further, the life cycle stage that emerges as the leading contributor to the total for each technology varies from technology to technology. For coal, natural gas, and hydrothermal flash, the dominant stage is fuel or geofluid use during plant operation. For nuclear and biomass, the fuel production stage is the largest GHG contributor to their respective life cycles. And for hydro, PV, wind, EGS, and hydrothermal binary, the plant cycle stage makes the largest GHG contribution. As expected, all generating technologies have GHG emissions from the plant cycle stage; see GHGpc/Eout values in Table A1. Interestingly, when compared to most of the renewable power technologies (biomass, wind, PV, and geothermal), plant-cycle energy and GHG emissions contributions to total life-cycle results are comparatively small for coal, NGCC, nuclear, and biomass thermoelectric systems. Where plant-cycle GHG emissions have the largest shares are for EGS geothermal and PV power generation, results that are fully consistent with their correspondingly high plant-cycle fossil energy consumption discussed above.

Comparing across all generating technologies, the "total" GHG values seen in Figure 16 show that fossil fuel plants generate the most GHGs per kWh, with all others yielding a small fraction of that amount. Hence, compared to fossil power plant totals, plant-cycle GHG emissions are small for all technologies. Although substantial GHG/kWh emissions are incurred in flash geothermal fuel use and biomass fuel production, their GHG emissions are still only 20% of those resulting from the most efficient fossil plant listed in the table (i.e., NGCC). When they are compared to coal, GHG emissions from flash geothermal and biomass fuel are less than 10%. With the possible exception of hydrothermal flash, geothermal systems are seen in Figure 16 to be among the lowest greenhouse gas emitters.

Regarding biomass-fueled electricity generation from forest residues, a significant amount of fossil energy is used in transporting the fuel to the plant and processing it for use. Further, incomplete combustion of the fuel in a biomass power plant is responsible for combustion methane emissions, which lead to a GHG emission for its fuel use stage. Also included in that value are N_2O emissions. Because of flash geothermal technology's direct use of the geofluid (vs. indirect use as in binary systems), most of the CO_2 dissolved in the fuel (geofluid), which had been geologically sequestered underground, is subsequently released into the atmosphere upon passing through the geothermal facility. It should be noted that CO_2 emissions associated with the geofluid vary depending upon the dissolved concentration, and an average value was assumed according to geothermal power plant emission data reported by Bloomfield et al. (2003).

6.4 COMPARISON OF CO_2 ESTIMATES WITH THOSE OF OTHER STUDIES

There are numerous energy and greenhouse gas emission studies of electricity production available in the literature. Some are complete LCAs, which include plant-cycle burdens, while others only cover some of the life cycle stages, typically the fuel use and production stages. Further, some of the LCA studies are process chain analyses, whereas others are "combined" studies, that is, a melding of results for process chain analyses and economic input/output data. A listing of some of those studies for the technology discussed herein is given in Table A2.

An inspection of the table reveals that about half of the studies are "combined" analyses, the other half being PCAs. In virtually all cases discussed in the previous sections where plant cycle energy and GHG emissions were estimated, the burdens for construction site energy consumption and for transportation of materials to the site could not be included because of a lack of available information. The combined approach allows for their being estimated, although their magnitudes are in question. Hence, it is widely accepted that the PCA method tends to underestimate LCA burdens, whereas the combined method tends to overestimate them. Clearly, the differences between the two approaches merit clarification (Fthenakis and Kim 2007).

Some of the references given in Table A2 cover a greater range of power-generating technologies than indicated there. For example, some of the coal studies explored the impact of carbon capture and sequestration. Because those technologies are not covered here, they have not been included in the table.

A comparison of our results (Table A1) with those in Table A2 is provided in Figure 17. Although some differences are evident, overall our results, which are averages of plant cycle stage GHG emissions added onto GREET-based fuel cycle energy and emission values, are in good accord with Table A2 results. First, our GHG emission value for coal is somewhat higher than the others. This result appears to be because of GREET's higher carbon content per MJ of coal versus those used in the other studies. One of the other differences shows a conspicuously high GHG value in the hydroelectric category. However, Gagnon and van de Vate (1997) advanced this estimate by considering GHG emissions, partly methane, arising from the decay of plant material, on the bottom of reservoirs behind hydro dams in very warm climates. Finally, the Argonne GHG value for biomass-based electric power is noticeably higher than are the others in that category. This finding is because of different biofuels. Argonne assumed forestry residues as the fuel, whereas the other assumed cultivated biomass crops, in this case willow and poplar.

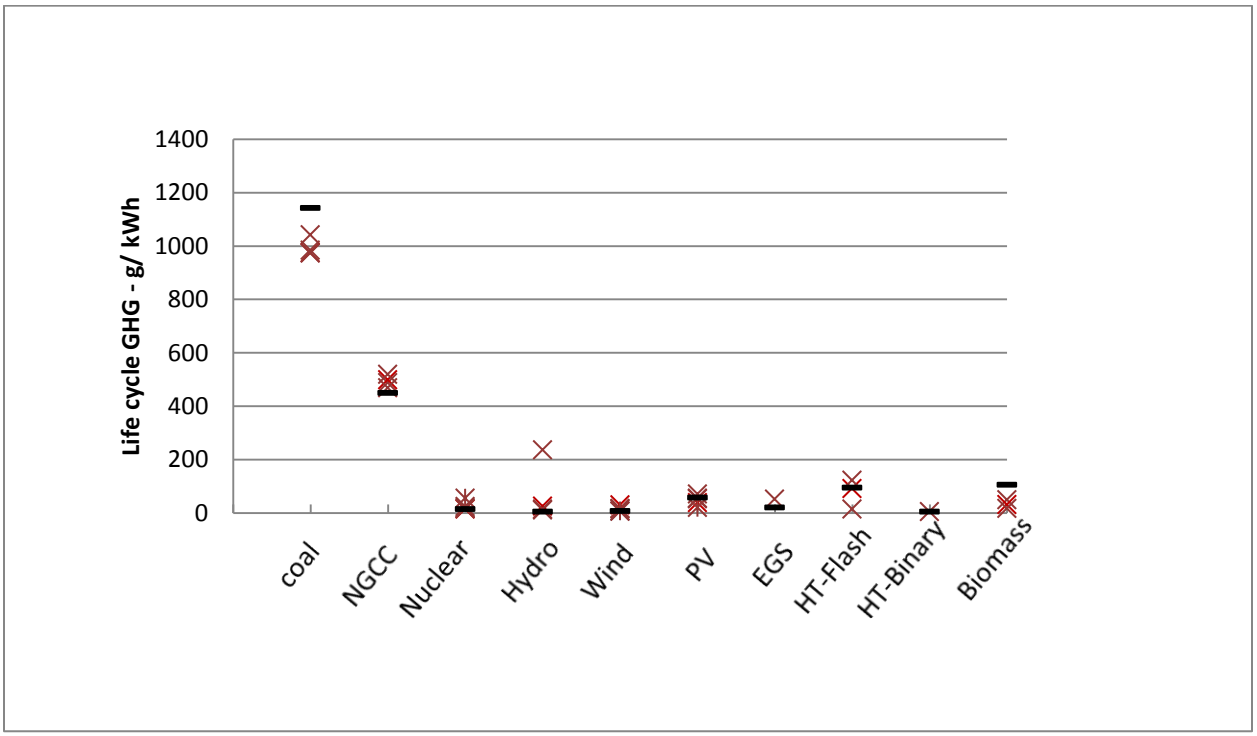

FIGURE 17 Greenhouse Gas Emissions for Electricity Production [(-) Argonne Average Values, (X) Literature Values]

When viewed on a category (power-generating technology) basis (see Table A2), considerable variation is observed in the results, especially those representing power systems where plant-cycle burdens dominate. In these cases, the magnitude of the GHG emissions is small in comparison to those of fossil plants. The reasons for the variation are multiple, including locale-specific factors, site design, study approach (combined vs. PCA), and study-to-study variations in available data. Despite wind technology GHG results, an inspection of Table A2 shows no consistent trend in which GHG emission results from "combined" studies tend to be higher than those derived from the PCA approach. This result is surprising. Because there is a

strong methodological reason to expect just such a trend, it appears that the other factors cited above are both significant and operative and, as such, are obscuring the distinction between the "combined" and PCA approaches.

7 CONCLUSIONS

A process-based life cycle energy and greenhouse gas emissions analysis was conducted for geothermal power-generating technologies, including enhanced geothermal systems, hydrothermal flash, and hydrothermal binary. Results from the analysis were compared to those from other electricity-generating technologies including coal, natural gas combined cycle, nuclear, hydroelectric, wind, photovoltaic, and biomass. Because of a scarcity of geothermal life cycle data, a scenario analysis approach was chosen for conducting this assessment. Because of the significant amounts of additional materials and construction energy required for drilling and constructing geothermal wells, a special emphasis has been placed on determining the contribution of the plant construction stage, termed herein the infrastructure stage (or plant cycle), of the life cycle to total energy consumption and carbon emissions for not only geothermal technologies but also the other power-generating technologies covered herein. Data for the plant cycle required for the LCA of the non-geothermal technologies included in this study were extracted from the literature.

From both our literature review and geothermal modeling, tables of material and energy requirements to build the various electricity-generating technologies were compiled. Further, the operational requirements and the energy required to provide them were also gathered for these technologies. It was found that the mass-to-power ratios (MPR in tonnes/MW) for materials such as the steel and concrete required to build and equip a power plant are the lowest for the conventional power systems (i.e., the thermoelectric systems), including coal, natural gas combined cycle, and nuclear. Biomass-to-power, a thermoelectric renewable system, shows the same material dependence. Other materials like copper and aluminum were tracked but are used in considerably smaller amounts in the conventional power systems. Renewable systems generally required more steel and concrete per MW capacity than do conventional systems. This finding is especially true for EGS and hydrothermal binary plants, a consequence which is attributed to the need for deeper wells and air-cooled condenser systems for the binary plants. Temperature of the resource also plays a role. For a given power output, a greater geofluid flow is required for lower-temperature resources, thus necessitating that more wells be built and hence, use of more cement and casings.

Further, the concrete MPR for gravity dams is (not surprisingly) quite high, and the steel and concrete MPRs for wind turbines are roughly two to five times higher than those of conventional systems. For some of the renewable systems, the aluminum MPR is much higher than it is for conventional systems. This result occurs because of the aluminum frames for photovoltaic arrays and heat-exchanger fins that are needed for the large air coolers in binary geothermal power systems.

Energy and GHG ratios for the infrastructure and other life cycle stages were also developed in this study to develop results for service functional unit (i.e., kWh). Energy burdens per energy output associated with plant infrastructure typically range from 2% to 6% for renewable power technologies, although PV can be as high as 50%. For conventional systems, the energy burden ranges from 0.1% to 0.3%. GHG emissions per energy output for plant construction follow a similar trend.

Total GHG emissions are by far the largest for fossil power plants and are much lower for the renewable power systems. GHG emissions that exist for renewable systems tend to be dominated by plant construction, although flash geothermal emissions are primarily attributable to fugitive GHGs from the geofluid during the plant operation stage of the life cycle. The GHG emissions for biomass plants are dominated by the fuel production life cycle stage. Despite the large amounts of steel and concrete required per MW power capacity, enhanced geothermal systems are one of the lower GHG emitters of the renewable systems studied per unit of lifetime kWh output. EGS GHG emissions can be reduced even further as well depth decreases. When compared to GHG emissions values from other studies, GREET model results are in good accord with them overall. The two outliers noted are readily explained on the basis of different fuel properties assumed. Relative variation among GHG study results is larger for power-generating technologies where plant-cycle burdens dominate.

Finally, the capability of the GREET model to provide rich energy detail for power generation from various technologies has been demonstrated. Further, the capability of the model has been expanded. The GREET model already contains modules for conventional and some renewable electric power-generating systems. Energy and GHG results developed for this study were developed by using GREET's existing modules and new prototype modules. As a result of this study, the model has been updated to include several new power-generating technologies, including enhanced geothermal, hydrothermal flash, and hydrothermal binary. Furthermore, through this study, the GREET model was expanded to include plant cycle, as well as fuel cycle, for life-cycle analysis of electric power generation systems.

8 REFERENCES

Asanuma, H., Y. Kumano, T. Izumi, N. Soma, H. Kaieda, K. Tezuka, D. Wyborn, and H. Niitsuma, 2004, "Passive Seismic Monitoring of a Stimulation of HDR Geothermal Reservoir at Cooper Basin, Australia," *SEG 2004 Expanded Abstracts*, 556–559.

Bertani, R., and I. Thain, 2001, *Geothermal Power Generating Plant CO2 Emission Survey*, Rev. 1.0, International Geothermal Association, Oct. [http://www.jeotermaldernegi.org.tr/ian%20i.htm], accessed August 2010.

Bloomfield, K.K., J.N. Moore, and R.M. Neilson, Jr., 2003, "Geothermal Energy Reduces Greenhouse Gases," *Climate Change Research*, March/April, 77–79.

Boustead, I., and G.F. Hancock, 1979, *Handbook of Industrial Energy Analysis*, Halstead Press, John Wiley and Sons.

Bryan, R.H., and I.T. Dudley, 1974, "Estimated Quantities of Materials in a 1000-Mwe PWR Power Plant," ORNL-TM-4515.

Burnham, A., M. Wang, and Y. Wu, 2006, "Development and Applications of GREET 2.7 – The Transportation Vehicle-Cycle Model," ANL/ESD/06-5, Center for Transportation Research, Argonne National Laboratory, Argonne, IL.

Caterpillar, 2009, *336D L Hydraulic Excavator*, AEHQ5990-02 (2-09) [http://xml.catmms.com/servlet/ImageServlet?imageId=C480968], accessed May 26, 2010.

CONCAWE/EUCAR/JRC (CONCAWE/European Council for Automotive R&D/European Commission Joint Research Centre), 2007, Well-to-Wheels Analysis of Future Automotive Fuels and Powertrains in the European Context: Well-to-Tank Report, Version 2c, March.

Clark, C.E., C.B. Harto, J.L. Sullivan, and M. Wang, 2010, *Water Use in the Development and Operations of Geothermal Power Plants*, Argonne National Laboratory, in process.

Delucchi, M.A., 2003, "A Lifecycle Emissions Model (LEM): Lifecycle Emissions from Transportation Fuels, Motor Vehicles, Transportation Modes, Electricity Use, Heating and Cooling Fuels, and Materials," Institute of Transportation Studies, University of California at Davis, Davis, CA, Dec.

de Wild-Schoulten, M.J., and E.S. Alsema, 2005, "Environmental Life Cycle Inventory of Crystalline Silicon Photovoltaic Module Production," presented at the MRS Fall Meeting, Boston, MA, ECN-RX-06-2005.

DynaCorp EENSP, Inc., 1995, "Assessment of the Environmental Benefits of Renewables Deployment: A Total Fuel Cycle Analysis of the Greenhouse Gas Impacts of Renewable Generation Technologies in Regional Utility Systems," prepared for the National Renewable Energy Laboratory, contract no. DE-AC02-83CH10093, May.

EIA (Energy Information Administration), 2010, *Annual Energy Outlook 2010*, Tables 85 and 101 [http://www.eia.doe.gov/oiaf/aeo/], accessed August 2010.

El-Bassioni, A.A., 1980, "A Methodology and Preliminary Database for Examining the Health Risks of Electricity Generation from Uranium and Coal Fuels," Oak Ridge National Laboratory, NUREG/CR-1539.

EPA (U.S. Environmental Protection Agency), 2004, *Exhaust and Crankcase Emission Factors for Nonroad Engine Modeling—Compression-Ignition*, NR-009c, EPA420-P-04-009, revised April 2004 [http://www.epa.gov/OMS/models/nonrdmdl/nonrdmdl2004/420p04009.pdf], accessed April 16, 2010.

European Commission, 1997d, ExternE. Germany.

E-Z Line Pipe Support Co., Inc., 2005, "Foundation Detail for Pipe Support Figure 510: 16-inch Diameter," *ezline-CD* [http://www.ezline.com/ezline-CD.zip], accessed May 10, 2010.

Frick, S., M. Kaltschmidt, and G. Schroeder, 2010, "Life Cycle Assessment of Geothermal Binary Power Plants using Enhanced Low-Temperature Reservoirs," *Energy*, 35, 5: 2281–2294.

Fthenakis, V.M., and H.C. Kim, 2007, "Greenhouse Gas Emissions from Solar Electric and Nuclear Power: A Life Cycle Study," *Energy Policy*, 35, 2549–2557.

Fthenakis, V.M., H.C. Kim, and E. Alsema, 2008, "Emissions from Photovoltaic Life Cycles," *Envir. Sci. Technol*., 42, 2168–2174.

Gagnon, L., and J.F. van de Vate, 1997, "Greenhouse Gas Emissions from Hydropower," *Energy Policy*, 25, 7–13.

Heller, M.C., G.A. Keoleian, M.K. Mann, and T.A. Volk, 2004, "Life Cycle Energy and Environmental Benefits of Generating Electricity from Willow Biomass," *Renewable Energy*, 29, 1023–1042.

Hondo, H., 2005, Life Cycle Greenhouse Gas Emission Analysis of Power Generating Systems: Japanese Case, *Energy* 30, 2042–2056.

IDOT (Illinois Department of Transportation), 2007, "Section 1019: Controlled Low-Strength Material (CLSM)," *Standard Specifications for Road and Bridge Construction*, 758–760.

ISO International Standard, 1997, "Environmental Management - Life Cycle Assessment - Principles and Framework," ISO/FDIS 14040.

ISO International Standard, 1998, "Environmental Management - Life Cycle Assessment - Goal and Scope Definition and Inventory Analysis," ISO 14041.

ISO International Standard, 2000, "Environmental Management - Life Cycle Assessment - Life Cycle Impact Assessment," ISO 14042.

Kendall, A., 2007, "Concrete Infrastructure Sustainability: Life Cycle Metrics, Materials Design, and Optimized Distribution of Cement Production," Report # CSS07-07, University of Michigan.

Keoleian, G.A., and G. McD. Lewis, 2003, Modeling the Life Cycle Energy and Environmental Performance of Amorphous Silicon BIPV Roofing in the U.S., *Renewable Energy*, 28, 271–293.

Mann, M.K., and P.L. Spath, 1997, "Life Cycle Assessment of Biomass Gasification Combined-Cycle System," DOE Contract Number DE-AC36-83CH10093.

Mansure, A.J., 2010, "Review of Past Geothermal Energy Return on Investment Analyses," *GRC Transactions 2010*.

Mason, J.M., V.M. Fthenakis, T. Hansen, and H.C. Kim, 2006, "Energy Pay-Back and Life Cycle CO2 Emissions of the BOS in an Optimized 3.5 MW PV Installation," *Prog. In Photovoltaics Res. and Applications*, 14; 179–190.

McAllister, E.W. (editor), 2009, "Spacing of Pipe Supports," *Pipeline Rules of Thumb Handbook, 7th Edition: A Manual of Quick, Accurate Solutions to Everyday Pipeline Engineering Problems*, Gulf Professional Publishing (Elsevier), May.

Meier, P.J., 2002, "Life Cycle Assessment of Electricity Generation Systems and Applications For Climate Change Policy," UWFDM-1181.

Michelet, S., and M.N. Toksöz, 2006, *Fracture Mapping in the Soultz-sous-Forêts Geothermal Field from Microearthquake Relocation*, Earth Resource Laboratory Consortium Report [http://eaps.mit.edu/erl/previous_reports.html#2006], accessed January 13, 2010.

MIT (Massachusetts Institute of Technology), 2006, *The Future of Geothermal Energy: Impact of Enhanced Geothermal Systems (EGS) on the United States in the 21st Century*, prepared under contract for the U.S. Government under D.O.E. Contract DE-AC07-05ID14517.

Narasimhan, T.N., and P.A. Witherspoon, 1977, "Reservoir Evaluation Tests on RRGE 1 and RRGE 2, Raft River Geothermal Project, Idaho," Lawrence Berkeley Laboratory, LBL-5958 [http://www.osti.gov/bridge/servlets/purl/7305201-Rik8v4/7305201.pdf], accessed April 1, 2010.

NUREG-1640, 2004, "Radiological Assessments for Clearance of Materials from Nuclear Facilities," Appendices A through E, Vol. 2.

Odeh, N.A., and T.T. Cockerill, 2008, "Life Cycle GHG Assessment of Fossil Fuel Power Plants with Carbon Capture and Storage," *Energy Policy*, 36, 367–380.

Pacca, S., and A. Horvath, 2002, "Greenhouse Gas Emissions from Building and Operating Electric Power Plants in the Upper Colorado River Basin," *Environ. Sci. & Technol*., 36, 3194–3200.

Phylipsen, G.P.M., and E.A. Alsema, 1995, "Environmental Life Cycle Assessment of Multi-Crystalline Silicon Solar Cell Modules," Report #95057, Department of Science, Technology and Society, Utrecht University, Netherlands.

Polsky, Y., L. Capuano, Jr., J. Finger, M. Huh, S. Knudsen, A.J. Mansure, D. Raymond, and R.J. Swanson, 2008, "Enhanced Geothermal Systems (EGS) Well Construction Technology Evaluation Report," Sandia Report SAND2008-7866.

Polsky, Y., A.J. Mansure, D. Blankenship, R.J. Swanson, and L.E. Capuano, Jr., 2009, "Enhanced Geothermal Systems (EGS) Well Construction Technology Evaluation Synopsis," *Proceedings Thirty-Fourth Workshop on Geothermal Reservoir Engineering*, SGP-TR-187.

Radback Energy, 2009, "Appendix 5.1E Construction Data," *Contra Costa Generating Station - Application for Certification*, Docket # 09-AFC-4, The California Energy Commission [http://www.energy.ca.gov/sitingcases/oakley], accessed August 2010.

Rule, B.M., Z.J. Worth, and C.A. Boyle, 2009, "Comparison of Life Cycle Carbon Dioxide Emissions and Embodied Energy in Four Renewable Electricity Generation Technologies in New Zealand," *Environ. Sci. & Technol*., 43, 6406–6413.

Schleisner, L., 2000, "Life Cycle Assessment of a Wind Farm and Related Externalities," *Renewable Energy*, 20, 279–288.

Sonoco Products Company, 2008, *Sonotube Concrete Forms Technical Leaflet* [http://sonotube.com/europe/docs/IPDEuro_techsheet_ENG.pdf], accessed January 27, 2010.

Spath, P.L., M.K. Mann, and D.R. Kerr, 1999, "Life Cycle Assessment of Coal-Fired Power Production," NREL/TP-520-25119.

Spath, P.L., and M.K. Mann, 2000, "Life Cycle Assessment of a Natural Gas Combined-Cycle Power Generation System," NREL/TP-570-27715.

Spitzley, D.V., and G.A. Keoleian, 2004, Life Cycle Environmental and Economic Assessment of Willow Biomass Electricity: A Comparison with Other Renewable and Non-Renewable Sources, a report of the Center for Sustainable Systems, University of Michigan, Report No. CSS04-05R.

Tester, J., et al., 2006, *The Future of Geothermal Energy: Impact of Enhanced Geothermal Systems (EGS) on the United States in the 21st Century*, Massachusetts Institute of Technology [http://geothermal.inel.gov/publications/future_of_geothermal_energy.pdf], accessed August 2010.

U.S. LCI Database, undated, Electricity Modules [http://www.nrel.gov/lci/database], accessed August 2010.

Vestas (Vestas Wind Systems A/S), 2006, "Life Cycle Assessment of Electricity Delivered from an Onshore Power Plant based on Vestas V82-1.65 MW Turbines," Dec. 29 [http://www.vestas.com/], accessed August 2010.

White, S.W., and G.L. Kulcinski, 1998a, "Birth to Death Analysis of the Energy Payback Ratio and CO_2 Gas Emission Rates From Coal, Fission, Wind and DT Fusion Electrical Power Plants," UWFDM-1063.

White, S.W., and G.L. Kulcinski, 1998b, "Net Energy Payback and CO_2 Emissions from He-3 Fusion and Wind Electrical Power Plants," UWFDM-1093.

White, S.W., 2007, "Net Energy Payback and CO_2 Emissions from Three Midwestern Wind Farms: An Update," *Nat. Resources Res*., 15, 271–281.

Wang, M., 1999, "GREET 1.5 – Transportation Fuel-Cycle Model," ANL/ESD-39, Center for Transportation Research, Argonne National Laboratory, Argonne, IL.

Zimmermann, G., I. Moeck, and G. Blocher, 2009, "Cyclic Waterfrac Stimulation to Develop an Enhanced Geothermal System (EGS) – Conceptual Design and Experimental Results," *Geothermics*.

APPENDIX: ENERGY RATIOS AND SPECIFIC CARBON GRAPHS

Please refer to Section 6, which provides discussion on Figures A1 through A6 and Tables A1 and A2.

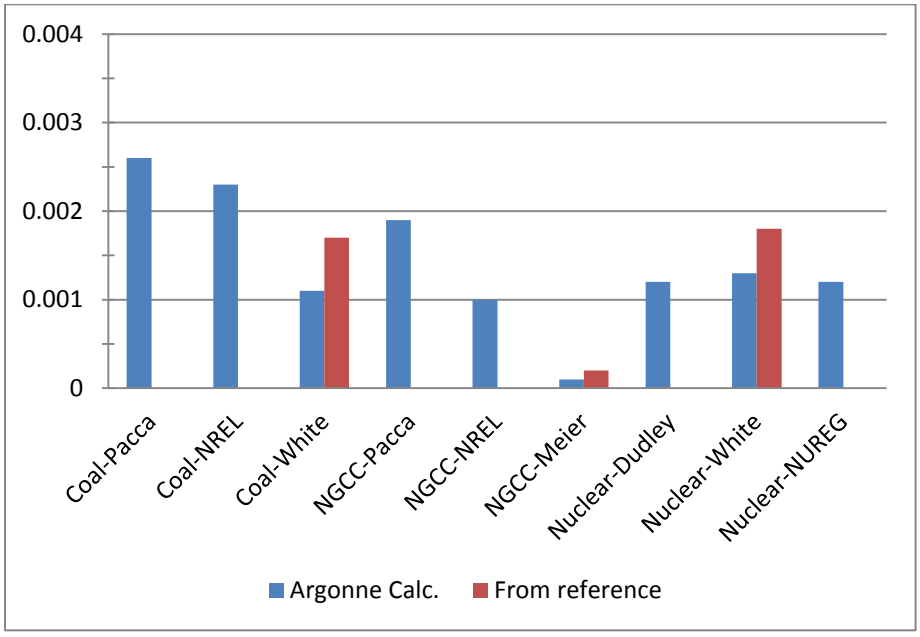

FIGURE A1 Energy Ratios for Conventional Power Plant, MJ_{pc}/MJ_{out}

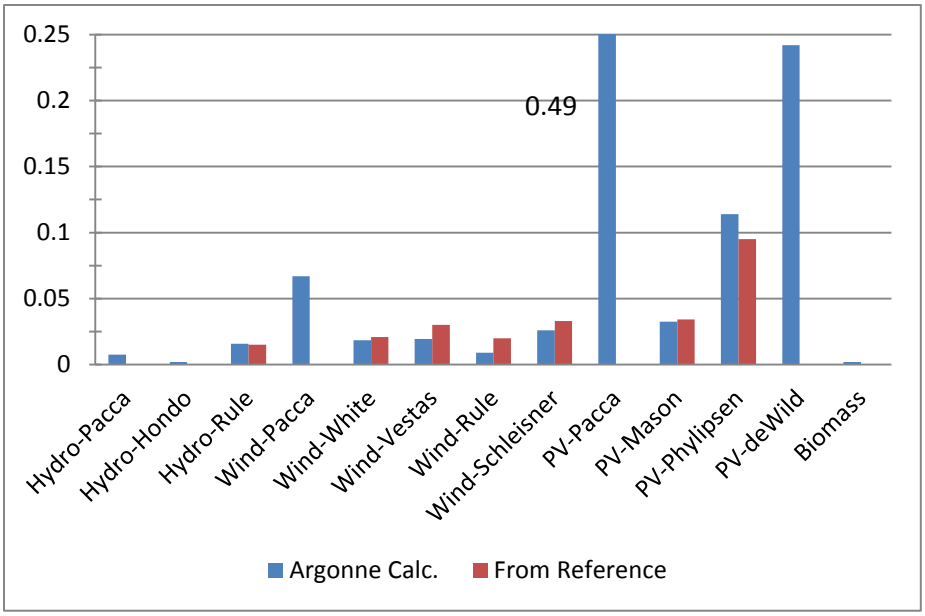

FIGURE A2 Energy Ratios for Renewable Electricity, MJ_{pc}/MJ_{out}

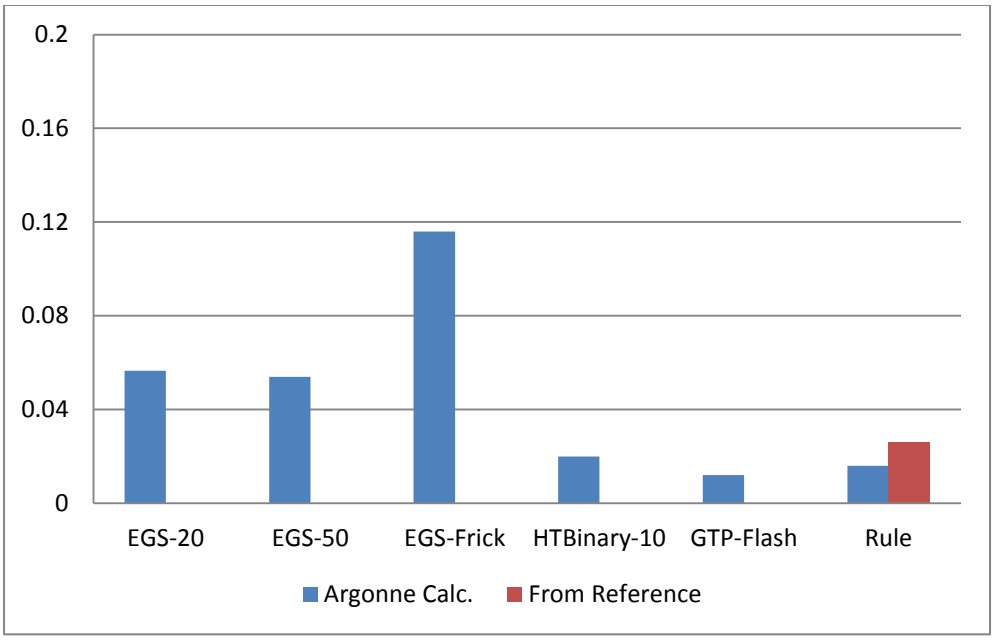

FIGURE A3 Energy Ratios for Geothermal Electric Power, MJ_{pc}/MJ_{out}

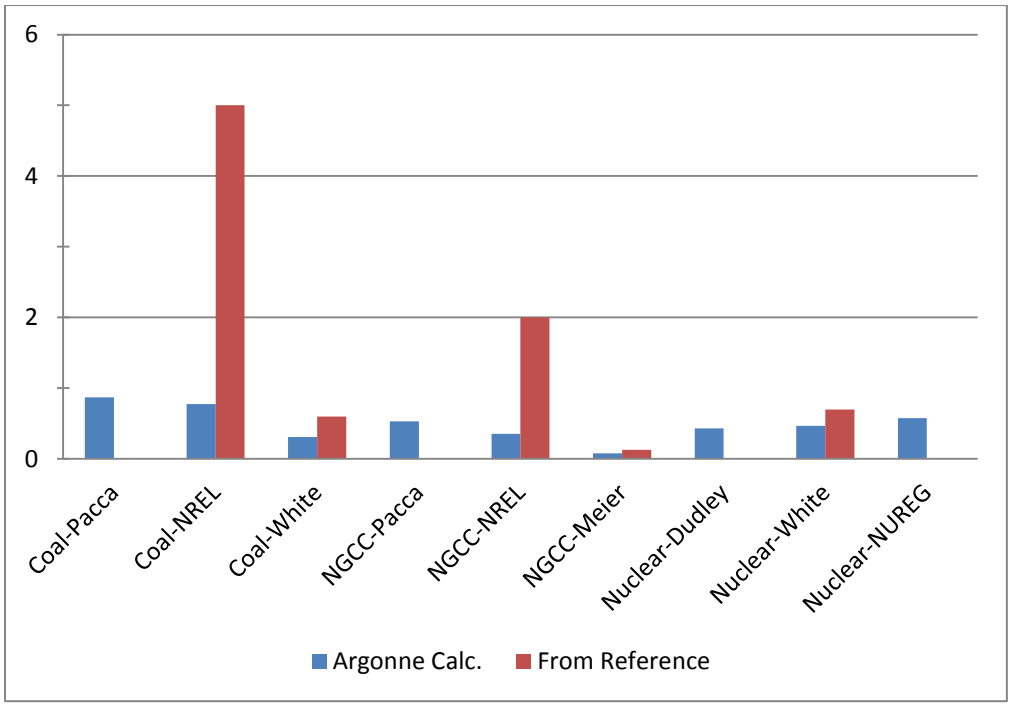

FIGURE A4 Specific Carbon for Conventional Electric Power, g GHG_{pc}/kWh_{out}

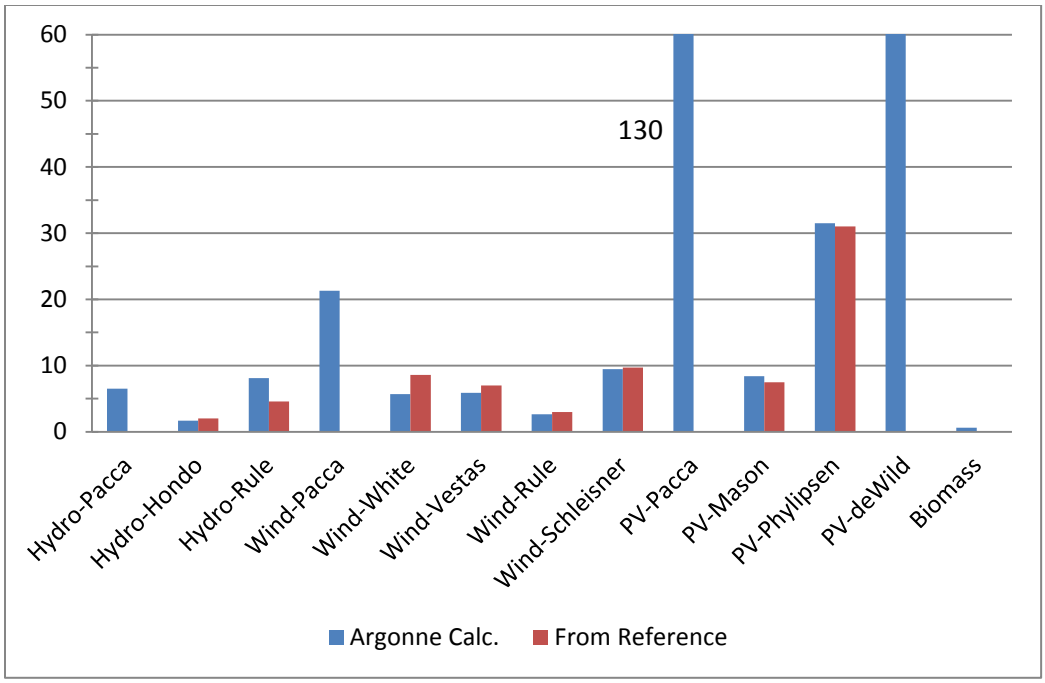

FIGURE A5 Specific Carbon for Renewable Power, g GHG_{pc}/kWh_{out}

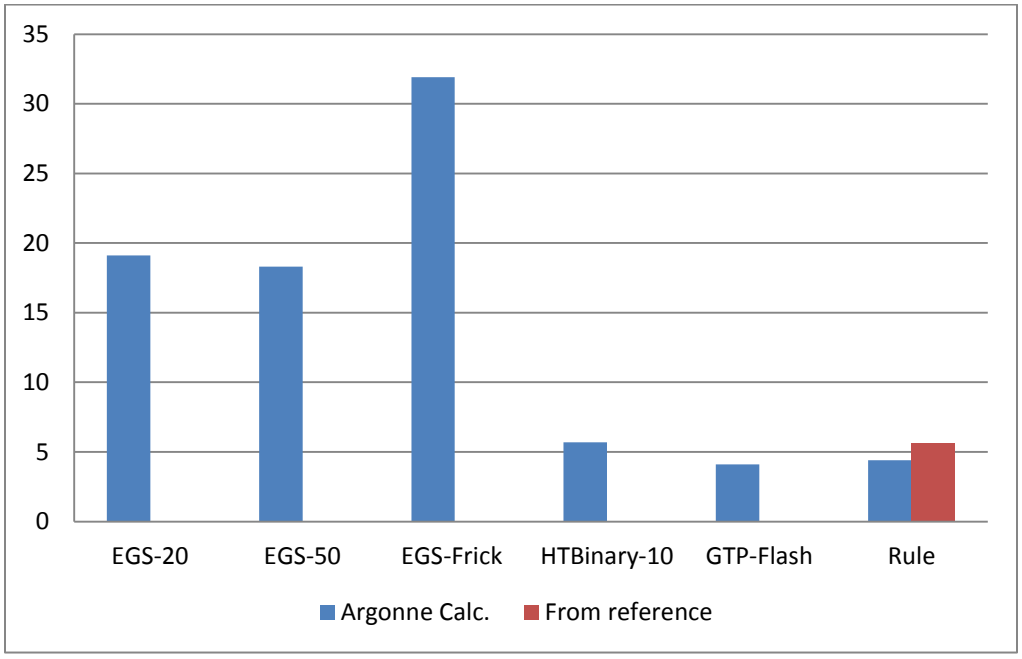

FIGURE A6 Specific Carbon for Geothermal Power, g GHG_{pc}/kWh_{out}

TABLE A1 PC Life Cycle Stage Energy Ratios (dimensionless) and Carbon Emissions (grams per kWh) for Various Power-Generating Technologies

	Coal	NGCC	Nuclear	Nuclear	Hydro	Wind	PV	Geothermal	Geothermal	Hydrothermal	Biomass
			PWR	BWR				EGS	Flash	Binary	
					Average						
E_{pc}/E_{out}	0.20%	0.10%	0.12%	0.12%	0.84%	2.48%	21.82%	7.52%	1.16%	2.05%	0.21%
GHG/E_{out}											
Infrastructure	0.7	0.3	0.5	0.6	5.4	8.0	62.3	23.0	4.1	5.7	0.6
Fuel production	50.4	67.2	16.0	16.0	0.0	0.0	0.0	0.0	0.0	0.0	73.8
Fuel use	1,183.8	419.5	0.0	0.0	0.0	0.0	0.0	0.0	98.9	0.0	40.6
Total	1,234.9	487.0	16.5	16.6	5.4	8.0	62.3	23.0	103.0	5.7	115.0
					Maximum						
E_{pc}/E_{out}	0.26%	0.19%	0.13%	0.12%	1.58%	6.73%	48.44%	11.6%	1.16%	2.05%	0.21%
GHG_{pc}/E_{out}	0.87	0.53	0.47	0.58	8.11	21.32	141.90	31.9	4.10	5.73	0.64
					Minimum						
E_{pc}/E_{out}	0.10%	0.01%	0.11%	0.12%	0.19%	0.90%	3.26%	5.39%	1.16%	2.05%	0.21%
GHG_{pc}/E_{out}	0.31	0.08	0.43	0.58	1.69	2.64	8.35	18.3	4.10	5.73	0.64

TABLE A2 GHG Emissions (g/kWh) from Various Power-Generating Technologies: PCA Denotes Process Chain Analysis and Combined Signifies both PCA and Economic Input/Output Analysis

Study	GHG/kWh	Comment	LCA Approach
Coal			
Spath et al., 1999 – Average	1,042	Ave 3 PCB[a], 360 MW, 60%CF[b], 30 CY[c]	PCA
Honda, 2005	975	1000 MW, 70% CF, 30 CY	Combined
White, 1998a	974	1000 MW, 75% CF, 40 CY	Combined
Odeh and Cockerill, 2008	984	Sub-crit PCB, 500 MW, 75%CF, 30CF	Combined
NGCC			
Odeh and Cockerill, 2008	488	500 MW, 75%CF, 30CF	Combined
Spath and Mann, 2000	499	505 MW, 80% CF	PCA
Hondo, 2005	519	1000 MW, 70% CF, 30 CY	Combined
Meier, 2002	469	620 MW, 75%CF, 40CY	Combined
Nuclear			
Hondo, 2005	24	BWR, 1000 MW, 70%CF, 30CY	Combined
White, 1998a	15	1000 MW, 75%CF, 40CY	Combined
European Commission, 1997, Germany	20	PWR 1375 MW, 90%CF, 40CY	PCA
Fthenakis & Kim, 2007	16 - 55		Combined
Hydroelectric			
Hondo, 2005	11	Run of River, 10 MW, 45% CF, 30 CY	Combined
Spitzley & Keoleian, 2004	26	Gravity Dam, 1296 MW	PCA
Gagnon & van de Vate, 1997	15 - 237	Plant details not given	PCA
Wind			
White, 1998a, 1998b	15	25 MW farm, 24% CF, 25 CY	Combined
Hondo, 2005	30	0.3 MW, 20% CF, 30 CY	Combined
European Commission, 1997, Germany	6	11.25 MW, 25% CF, 20 CY	PCA
Schleisner, 2000	10 - 17	5 & 9 MW, 29% CF, 20 CY	PCA
Vestas, 2006	7	300 MW farm, 41% CF, 20 CY	PCA
White, 2007	14 - 34	1.2 to 108 MW, CF = 20%-29%, 25-30 CY	Combined
Solar			
Hondo, 2005	53	BIPV[d] 3kW, 15% CF, 30 CY	Combined
Meier, 2002	39	BIPV 8 kW, 20% CF, 30 CY	Combined
European Commission, 1997, Germany	55	BIPV, 4.8 kW, 8.3% CF, 25 CY	PCA
Spitzley & Keoleian, 2004	44 - 71	Amorphous Si BIPV, 20 CY	PCA
Fthenakis et al., 2008	21 - 54	30 CY	Combined
Geothermal			
Hondo, 2005	15	55 MW Flash plant, 60% CF, 30 CY	Combined
Bloomfield	91	Flash: fluid only	PCA
Bertani & Thain, 2001	4 – 740	Flash: fluid only, Range	PCA
"	122	Flash, Weighted Average	PCA
Frick et al., 2010	52	EGS Power only, 0.93 MW, 30 CY	PCA
Rule et al., 2009	5.6	HT binary, 162 MW, 93% CF, 100 CY	PCA
Biomass			
Spitzley & Keoleian, 2004	32	Willow – Direct Fire	PCA
European Commission, 1997, France	17	Fuel Cycle	PCA

[a] Pulverized coal boiler.
[b] Capacity factor.
[c] Calendar years of useful life.
[d] Building integrated photovoltaic.

Energy Systems Division
Argonne National Laboratory
9700 South Cass Avenue, Bldg. 362
Argonne, IL 60439-4815

www.anl.gov